

8-7-2004

Role of Actin Cytoskeleton Filaments in Mechanotransduction of Cyclic Hydrostatic Pressure

Keertik S. Fulzele

Follow this and additional works at: <https://scholarsjunction.msstate.edu/td>

Recommended Citation

Fulzele, Keertik S., "Role of Actin Cytoskeleton Filaments in Mechanotransduction of Cyclic Hydrostatic Pressure" (2004). *Theses and Dissertations*. 3832.
<https://scholarsjunction.msstate.edu/td/3832>

This Graduate Thesis - Open Access is brought to you for free and open access by the Theses and Dissertations at Scholars Junction. It has been accepted for inclusion in Theses and Dissertations by an authorized administrator of Scholars Junction. For more information, please contact scholcomm@msstate.libanswers.com.

ROLE OF ACTIN CYTOSKELETON FILAMENTS IN MECHANOTRANSDUCTION
OF CYCLIC HYDROSTATIC PRESSURE

By

Keertik Fulzele

A Thesis
Submitted to the Faculty of
Mississippi State University
in Partial Fulfillment of the Requirements
for the Degree of Master of Science
in Biomedical Engineering
in the Department of Agriculture and Biological Engineering

Mississippi State, Mississippi

August 2004

ROLE OF ACTIN CYTOSKELETON FILAMENTS IN MECHANOTRANSDUCTION
OF CYCLIC HYDROSTATIC PRESSURE

By

Keertik Fulzele

Approved:

Steven H. Elder
Associate Professor of Biological
Engineering
(Director of Thesis)

Robert C. Cooper Jr.
Professor and Associate Dean and Head
Clinical Sciences Department
(Committee Member)

Robert P. Taylor
Interim Dean
College of Engineering

Joel D. Bumgardner
Interim Department Head of Biological
and Agricultural Engineering
Graduate Coordinator of Biomedical
Engineering Program
(Committee Member)

John R. Welborn
Assistant Professor of Biological
Sciences
(Committee Member)

Name: Keertik S. Fulzele

Date of Degree: August 7, 2004

Institution: Mississippi State University

Major Field: Biomedical Engineering

Major Professor: Dr. Steven H. Elder

Title of Study: ROLE OF ACTIN CYTOSKELETON FILAMENTS IN

MECHANOTRANSDUCTION OF CYCLIC HYDROSTATIC PRESSURE

Pages in Study: 94

Candidate for Degree of Master of Science

Abstract:

This research examines the role of actin cytoskeleton filaments in chondroinduction by cyclic hydrostatic pressurization. A chondroinductive hydrostatic pressurization system was developed and characterized. A pressure of 5 MPa at 1 Hz frequency, applied for 7200 cycles (4 hours intermittent) per day, induced chondrogenic differentiation in C3H10T1/2 cells while 1800 cycles (1 hour intermittent) did not induce chondrogenesis. Quantitative analysis of chondrogenesis was determined as sulfated glycosaminoglycan synthesis and rate of collagen synthesis while qualitative analysis was obtained as Alcian Blue staining and collagen type II immunostaining. Actin disruption using 2 μ M Cytochalasin D inhibited the enhanced sGAG synthesis in the chondroinductive hydrostatic pressurization environment and significantly inhibited rate of collagen synthesis to the mean level lower than that of the non-pressurized group.

These results suggest an involvement of actin cytoskeleton filaments in mechanotransduction of cyclic hydrostatic pressure.

Keywords: Chondrogenesis; Mesenchymal stem cell; Hydrostatic pressurization; Actin cytoskeleton filaments

DEDICATION

To Prateek, Rasik, Mom, Dad and Sami.

ACKNOWLEDGMENTS

I would like to express my sincere appreciation to those who have contributed to this thesis, without whose help it would not have been possible. First, I'd like to thank the Department of Agriculture and Biological Engineering for providing the funding for not only this project, but also for my graduate education thus far. I express the utmost gratitude to Dr. Steven H. Elder who has served as my major professor and committee chairman and has provided unmatched guidance throughout my graduate education and the thesis process. Many thanks are also due to Dr. Joel D. Bumgardner, Dr. John R. Welborn and Dr. Robert C. Cooper, Jr. who have all served as members of my thesis committee and have given their invaluable time and advice throughout the process. I would also like to thank Mr. William A. Monroe, Electron Microscopist of the Mississippi State University Electron Microscopy Center, for his help on confocal microscopy imaging. I would like to thank the staff of the Department of Agriculture and Biological Engineering who has provided much appreciated services. Last but not the least; I would like to thank my laboratory colleagues and graduate students for being such wonderful friends and making my stay at the Mississippi State University such an enjoyable and memorable experience.

TABLE OF CONTENT

	Page
DEDICATION	ii
ACKNOWLEDGEMENTS	iii
LIST OF TABLES	vii
LIST OF FIGURES	x
CHAPTER	
I.INTRODUCTION AND REVIEW OF LITRATURE.....	1
The Promises of Tissue Engineering	2
Articular cartilage injuries	6
Articular Cartilage Anatomy and Physiology.....	7
Biomechanics of articular cartilage	9
Cell Differentiation and Chondrogenesis.....	11
Principles of Cell Mechanics for Cartilage Tissue Engineering.....	14
Mechanisms for Mechanotransduction	15
Role of Cytoskeleton.....	16
Mechanotransduction and cytoskeleton	19
Tools for Cytoskeleton Study	21
Gene Expression and Growth Factors.....	22
Statement of Hypothesis	24
II.METHODS AND MATERIALS.....	25
Experimental Design Outline.....	25
Materials and Methods.....	29

CHAPTER	Page
Chemicals.....	29
BMP-2.....	29
Cytochalasin-D	29
Cell Culture.....	29
C3H/10T1/2	29
For Study of Cytoskeletal Elements	30
For Cytotoxicity Studies	31
For Actin Disruption Studies	32
For Actin Disruption Induced Chondrogenesis Studies.....	32
Chondrogenic Effect of Hydrostatic Pressurization	33
Effect of Actin Disruption on Chondrogenesis by Hydrostatic Pressurization	35
Pressurization System	35
Immunofluorescence.....	36
Assessment of Chondrogenesis.....	38
DNA Quantification.....	38
Sulfated Glycosaminoglycan Quantification	38
Rate of Collagen Synthesis	39
Collagen Type II Immunostaining.....	40
Alcian Blue and Toluidine Blue Staining	40
Statistics	41
 III.RESULTS	 42
Actin filaments: Immunofluorescence Visualization.....	42
Cytotoxicity Evaluation of Cytochalasin D	44
Cytochalasin D Induced Disruption of Actin Filaments.....	46
Reversible Effect of Cytochalasin D.....	49
Chondrogenic Effects of Actin Disruption	50
Immunofluorescence.....	50
Toluidine Blue Staining of Glycosaminoglycan (Qualitative Analysis)	53
Statistical Analysis of Sulfated Glycosaminoglycan (Quantitative Analysis)	54
Chondrogenic Effects of Short Duration Hydrostatic Pressurization.....	56
Statistical Analysis for sGAG/DNA	56
Statistical Analysis: Rate of Collagen Synthesis	59
Collagen Type II Immunostaining.....	61
Alcian Blue Staining.....	62
Chondrogenic Effects of Long Duration Hydrostatic Pressurization	63
Statistical Analysis for sGAG/DNA	63
Statistical Analysis: Rate of Collagen Synthesis	65
Collagen Type II Immunostaining.....	67
Alcian Blue Staining.....	68

CHAPTER	Page
Effect of Actin Disruption (by Cytochalasin D) on Chondrogenic Effects of Long Duration Hydrostatic Pressurization	69
Statistical Analysis for sGAG/DNA	69
Statistical Analysis: Rate of Collagen Synthesis	71
Collagen Type II Immunostaining	73
Alcian Blue Staining	74
IV.DISCUSSION AND CONCLUSION.....	75
REFERENCES CITED.....	82
APPENDIX	
A. HYDROSTATIC PRESSURIZATION DEVICE	91

LIST OF TABLES

TABLE		Page
1.1	Differentiation Potential of Bone Marrow-Derived Mesenchymal Progenitors in-vitro: Stimuli, Molecular and Cellular Markers.....	13
3.1	Toxicity effects of varying concentration of Cytochalasin D on C3H10T1/2 cells	44
3.2	Linear correlation model for evaluating cytotoxicity of Cytochalasin D on C3H10T1/2 cells	45
3.3	Effects of various concentrations of Cytochalasin D on cell shape (actin disruption) in Chick Limb Bud Cells.....	47
3.4	Two-way ANOVA table for sGAG/DNA readings analyzing chondroinductive effect of BMP-2 and Cytochalasin D.....	54
3.5	Student's t-test for sGAG/DNA readings, comparing population means for control (non-pressurized) and experimental (pressurized) independent samples, analyzing chondroinductive effect of short duration hydrostatic pressurization.....	57
3.6	F-test for radioactive counts per minute readings, comparing population standard deviations for control (non-pressurized) and experimental (pressurized) independent samples, analyzing chondroinductive effect of short duration hydrostatic pressurization...	57

TABLE	Page
3.7 Student's t-test for radioactive counts per minute readings, comparing means for control (non-pressurized) and experimental (pressurized) independent samples, analyzing rate of collagen synthesis of C3H10T1/2 cells subjected to short duration hydrostatic pressurization	60
3.8 F-test for radioactive counts per minute readings, comparing population standard deviations for control (non-pressurized) and experimental (pressurized) independent samples, analyzing rate of collagen synthesis of C3H10T1/2 cells subjected to short duration hydrostatic pressurization.....	60
3.9 Student's t-test for sGAG/DNA readings, comparing means for control (non-pressurized) and experimental (pressurized) independent samples, analyzing chondroinductive effects of long duration hydrostatic pressurization	63
3.10 F-test for sGAG/DNA readings, comparing population standard deviations for control (non-pressurized) and experimental (pressurized) independent samples, analyzing chondroinductive effect of long duration hydrostatic pressurization	65
3.11 Student's t-test for radioactive counts per minute readings, comparing means for control (non-pressurized) and experimental (pressurized) independent samples, analyzing rate of collagen synthesis in long duration hydrostatic pressurization	66
3.12 F-test for radioactive counts per minute readings, comparing population standard deviations for control (non-pressurized) and experimental (pressurized) independent samples, analyzing rate of collagen synthesis of C3H10T1/2 cells subjected to long duration hydrostatic pressurization	66

TABLE	Page
3.13 Student's t-test for sGAG/DNA readings for control (non-pressurized) and experimental (pressurized with Cytochalasin D) samples, subjected to long duration hydrostatic pressurization	70
3.14 F-test for sGAG/DNA readings for control (non-pressurized) and experimental (pressurized with Cytochalasin D) independent samples, subjected to long duration hydrostatic pressurization.....	70
3.15 Student's t-test for radioactive counts per minute readings, comparing means for control (non-pressurized) and experimental (pressurized with Cytochalasin D) independent samples, analyzing rate of collagen synthesis of actin disrupted C3H10T1/2 cells subjected to long duration hydrostatic pressurization.....	72
3.16 F-test for radioactive counts per minute readings, comparing population standard deviations for control (non-pressurized) and experimental (pressurized with Cytochalasin D) independent samples, analyzing rate of collagen synthesis of actin disrupted C3H10T1/2 cells subjected to long duration hydrostatic pressurization	72

LIST OF FIGURES

FIGURE	Page
1.1 Four zones of articular cartilage	8
1.2 Strains produced in various loading conditions	10
1.3 Mesenchymal Stem Cell Differentiation: Steps and Terminal Cell Types	12
1.4 Microtubule structure in transformed cells	17
1.5 Actin (red) and microtubule (green) structures shown in cow endothelial cells. The nucleus is stained blue	22
2.1 Experimental design flow-diagram.....	26
2.2 Schematic drawing of device for applying cyclic hydrostatic compression to cultured cells.....	36
3.1 Immunofluorescence visualization of actin filaments (red in color) and tubulin filaments (green in color) (A) 400 magnification (B) 630 magnification	43
3.2 Standard Curve using CellTiter 96® AQueous One Solution Cell Proliferation Assay.....	44
3.3 Cytochalasin D cytotoxicity readings scatter plot	45
3.4 Effect of various concentrations of Cytochalasin D on actin disruption in C3H10T1/2 cells treated for 2 hr. (400 magnification). Smooth and continuous actin fibers (A; Control) are compared with Cytochalasin D induced actin disruption with progressive concentrations (B, C and D; 2, 4, 8 μ M Cytochalasin D respectively).....	48

FIGURE	Page
3.5 Reversible effect of Cytochalasin D on actin disruption. (A) Effect of Cytochalasin D on actin disruption in C3H10T1/2 cells treated for 24 hr. (B) Actin reorganization in Cytochalasin D treated C3H10T1/2 cells 24 hr after removal of drug.....	49
3.6 Phalloidin-Propidium Iodide staining of C3H10T1/2 cells after 48 hours micromass culture. (A) Control (no BMP-2 or Cytochalasin D) 100 magnification at the center of micromass. (B) Control (no BMP-2 or Cytochalasin D) 400 magnification at the edge of micromass.....	51
3.7 Phalloidin-Propidium Iodide staining of C3H10T1/2 cells after 48 hours micromass culture. (A) BMP-2, 100 magnification at center. (B) BMP-2, 400 magnification at the edge	52
3.8 Phalloidin and Propidium Iodide staining of Cytochalasin D treated C3H10T1/2 cells after 48 hours in micromass culture. (A) Continuous exposure to 4 μ M Cytochalasin D, (100 magnification). (B) Initial 24-hour exposure to 4 μ M Cytochalasin D, (100 magnification).....	52
3.9 Day 12 toluidin-blue stained cultures (40 magnification). (A) Control, (B) BMP-2, (C) Continuous exposure to Cytochalasin D, (D) Continuous exposure to BMP-2 and Cytochalasin D.....	53
3.10 Means plot for sGAG/DNA readings analyzing chondroinductive effect of BMP-2 and Cytochalasin D.....	55
3.11 Interaction plot for BMP-2 and Cytochalasin D with respect to chondroinductive effect measured as sGAG/DNA	55
3.12 The sample distribution plots for sGAG/DNA readings comparing control (non-pressurized) and experimental (pressurized) groups subjected to short duration hydrostatic pressure. (A) Histogram (B) Box-and-whisker plot	58
3.13 Collagen type II immunostaining in micromass cultures of C3H/10T1/2 cells. A-B: Control, C-D: pressurized. Primary antibody was omitted from A and C	61

FIGURE	Page
3.14 Alcian blue histochemical staining for glycosaminoglycan in samples for testing chondroinductive effect of short duration hydrostatic pressurization. (A) Control (non-pressurized) (B) Experimental (Pressurized).....	62
3.15 The sample distribution plots for sGAG/DNA readings comparing control (non-pressurized) and experimental (pressurized) groups subjected to long duration hydrostatic pressure. (A and C) Box-and-whisker plot, (B and D) Histogram. (A and B) with outliers, (C and D) without outliers	64
3.16 Collagen type II immunostaining in micromass cultures of C3H/10T1/2 cells hydrostatically pressurized for long duration (4X). A-B: Control, C-D: pressurized. Primary antibody was omitted from A and C	67
3.17 Alcian blue histochemical staining for glycosaminoglycan in samples for testing chondroinductive effect of long duration hydrostatic pressurization. (A) Control (non-pressurized) (B) Experimental (Pressurized)	68
3.18 The sample distribution plots for sGAG/DNA readings comparing control (non-pressurized) and experimental (pressurized with Cytochalasin D) groups subjected to long duration hydrostatic pressure. (A) Box-and-whisker plot, (B) Histogram	71
3.19 Collagen type II immunostaining in micromass cultures of Cytochalasin D treated C3H/10T1/2 cells hydrostatically pressurized for long duration (4X). A-B: Control, C-D: pressurized. Primary antibody was omitted from A and C	73
3.20 Alcian blue histochemical staining for glycosaminoglycan in samples for testing chondroinductive effect of long duration hydrostatic pressurization with actin cytoskeleton elements disrupted using Cytochalasin D. (A) Control (non-pressurized) (B) Experimental (Pressurized with Cytochalasin D)	74
A.1 The hydrostatic pressurization chamber	91

FIGURE	Page
A.2 The hydrostatic pressurization chamber and control chamber was maintained in water bath at 37°C during pressurization.....	92
A.3 The overall setup of hydrostatic pressurization chamber with MTS machine controlled pressurization. Continuous water column was maintained from MTS machine to the pressurization chamber	93

CHAPTER I

INTRODUCTION AND REVIEW OF LITRATURE

Nationally, more than 80,000 men, women and children are awaiting an organ transplant; approximately 16 will die each day without receiving one. The waiting list is growing three times faster than the rate of organ donation (Center for Organ Recovery and Education website). The situation in developing and underdeveloped countries is even more alarming. Worldwide organ replacement therapies utilizing standard organometallic devices consume 8 percent of medical spending or approximately \$350 billion per year [Lysaght and O'Loughlin, 2000].

However, the organometallic devices do not impart the same quality of function as that of the damaged tissue or organ. Similar is the case with the other modes of treatment, which include organ transplant, surgical repair and drug therapy. Drawbacks of organ transplantation not only include a shortage of donor, but the recipients must have to remain on costly immunosuppressive drugs for the balance of their lives. Statistics have shown that over the years, the survival rates for major organ transplants are poor despite their high cost of maintenance. Surgical repairs are often imperfect and generally require multiple operations. The physical pain and discomfort associated with surgery and the psychological trauma of repeated operations is quite discouraging. Drug therapy is

generally associated with unwanted side effects. Gene therapy is showing promise; however, the efficiency of gene transfer and gene expression are major concerns at the forefront of gene therapy research. Engineered replacement organs could sidestep many of the hazards and problems associated with existing therapies, and at lower cost.

The Promises of Tissue Engineering

Tissue engineering aims at repairing or replacing damaged tissue or organs by delivering scaffolds with implanted cells, DNA, growth factors and other proteins at surgery. Dramatic advances in the fields of biochemistry, cell and molecular biology, genomics, biomedical engineering, chemical engineering, clinical practices, computational biology and materials science have given rise to the remarkable new cross-disciplinary field of tissue engineering. Although cells have been cultured, or grown, outside the body for many years, the possibility of growing complex, three-dimensional tissues and literally replicating the design and function of human tissue is the outcome of recent developments in this cross-disciplinary field of tissue engineering. The NSF Workshop on Tissue Engineering (1988) defined tissue engineering as “the application of principles and methods of engineering and life sciences toward fundamental understanding of structure-function relationships in normal and pathological mammalian tissues and the development of biological substitutes to restore, maintain, or improve tissue functions”. The definition can be modified on broader terms in modern times as the development and manipulation of laboratory-grown cells, tissues, or organs to replace or support the function of damaged or defective body parts.

Tissue engineering encompasses several sciences and technologies to work together. One strategy is using naturally occurring materials, like collagen, or synthetic materials, like polyglycolide (PGA), to fashion anatomically shaped "scaffolds" that are seeded with cells- from the patient or those of a donor. The cells seeded can include skin, muscle, cartilage, bone marrow, endothelial cells or more versatile stem cells which can give rise to many types of cells in the body. The entire structure of cells and scaffold is then implanted in the body at the site of injury where the scaffold provides a template that allows the cells to grow, reorganize and form new tissues. At the same time, the scaffold, being biodegradable, is gradually absorbed leaving a completely natural final product in the body. A less intense strategy involves injecting or placing proteins, such as growth factor, in the tissue that needs repairing. The protein then attracts the body's own cells to migrate into tissue and regenerate the tissue.

In May 1998 Apligraf®, the first tissue engineered organ (skin) developed by Organogenesis Inc, Canton, Massachusetts, was approved by the U.S. Food and Drug Administration. The product had great success in patients with burns or diabetic ulcers and in those undergoing dermatological surgery. The need for skin is acute: every year 600,000 Americans suffer from diabetic ulcers, which are particularly difficult to heal; another 600,000 have skin removed to treat skin cancer and between 10,000 and 15,000 undergo skin grafts to treat severe burns (Mooney and Mikos, 1999). In addition to skin, bone and cartilage are the first success stories of tissue engineering. Genzyme Tissue Repair in Cambridge, Massachusetts, has received FDA approval to engineer tissue derived from a patient's own cells for the repair of traumatic knee-cartilage damage.

Puelacher et al. (1994) have shown that anatomically shaped three-dimensional neocartilage can be grown subcutaneously in nude mice using a biodegradable polymer scaffold as a cell growth guide. Dean et al. (1999) have demonstrated that seeding biodegradable polymers with autologous bone marrow can grow new bone tissue.

Engineering of larger and more complex organs such as livers, kidneys, hearts, breasts, bladders and intestines, all of which include different kinds of cells, is at least theoretically possible. Griffith et al. (1997) have discussed the key design issues for *in-vitro* organogenesis of vascularized hepatic tissue and described a fabrication approach for making complex degradable polymer scaffolds to organize cells in three dimensions on the scale of hundreds of microns, and demonstrated the feasibility of using these scaffolds for *in-vitro* tissue organization in mixed-cell cultures. Many other advances are being made in the engineering of hearts, blood vessels, livers, pancreas and muscles.

Although there has been success in *in-vitro* synthesis of a few neo-organs like cartilage, the mechanical properties of these tissues are inferior to the natural tissues. For practical purposes the neo-tissues should have the same mechanical properties as that of the particular organ which can be specific to age, weight and sex of the patient. For example, the bones of a child and an adult differ in their mechanical properties. Also, the tissues in body are subjected to mechanical forces like shear forces in blood vessels.

Many tissues remodel or change their overall organization in response to the mechanical forces. Parkkinen et al. (1993) showed that cyclic hydrostatic pressures of physiological magnitude at 0.25 to 0.5 Hz frequencies have significantly increased proteoglycan synthesis in articular cartilage chondrocytes. Bonassar et al. (2001) found

that cartilage explants subjected to dynamic compression in the presence of insulin-like growth factor-I increased protein and proteoglycan synthesis by 180% and 290%, respectively. The influence of the combination of mechanical-growth factor stimulus was greater than that achieved by either of these factors alone.

Further *in-vivo* data and *in-vitro* research is required in order for tissue engineers to design neo-organs, particularly those that serve a predominantly biomechanical function. *In-vivo* stress and strain histories and mechanical failure conditions must be studied for a tissue subjected to different activities and then the mechanical standard must be set for the tissue to be engineered. *In-vitro* studies on single cells are required to understand how the physical forces influence cellular activity, cell-cell communication and cell-matrix communication.

The focus of this thesis is articular cartilage, which is avascular, aneural and made of a single cell type, chondrocyte, which produces extensive extracellular matrix. Since articular cartilage serves a mechanical function, the mechanical signals are modulators of cartilage regeneration. Although mechanical forces are known to stimulate chondrogenic differentiation of mesenchymal stem cells and production of cartilaginous matrix, as shown by many studies (Elder et al., 2001; Parkkinen et al., 1993; Bonassar et al., 2001), there is a fundamental lack of understanding of what mechanical stimuli are necessary to promote growth, differentiation and extracellular matrix synthesis. Also, how these mechanical signals are interpreted at the cellular level is still unclear. To attain this information, it is important to understand exact mechanical properties of the cell and their relationship to the local microenvironment and mechanism of mechanotransduction.

Articular cartilage injuries

Articular cartilage is an avascular, aneural, alymphatic tissue and therefore lacks the natural healing or restorative ability. Because it is aneural, it is possible for the articular cartilage to be damaged without the patient noticing any pain. Various degenerative cartilage conditions and/or acute trauma to musculoskeletal tissues can cause medical suffering to a widespread population.

Osteoarthritis, a gradual weakening of the cartilage that allows the joint to move fluidly, is caused by overuse, acute trauma, injury or obesity. The condition affects the knees, ankles, and fingers most frequently. The condition leads to a stiff, painful joint, with significant loss of range of motion. At times, osteoarthritis may cause small pieces of cartilage to break off and float around within the joint. It has become apparent that anabolic and catabolic mediators, released from chondrocytes themselves or from other joint cells, drive both destructive and repair activities in the osteoarthritic joint (van der Kraan and van den Berg WB, 2000).

The other common injuries of cartilage due to mechanical loading are chondral fracture i.e. articular cartilage (chondral) fracture; chondromalacia i.e. Softening of the articular cartilage; osteochondral fracture in which articular cartilage break off along with a piece of the underlying bone. Diseases of collagen fibers like chondrodysplasia arise due to over-expression of normal type II collagen (Garofalo et al., 1993) or genetic defects.

Current treatments of articular cartilage diseases, mostly surgical, alleviate the symptoms of the disease or restore some functions to the damaged tissue, but cannot

otherwise address the issue of healing articular cartilage. The lack of normal healing makes the regeneration of functional articular cartilage a very challenging job for bioengineers who must find alternative ways of stimulating cartilage growth.

Articular Cartilage Anatomy and Physiology

Articular cartilage is the connective tissue in the knee that covers the femur, the tibia, and the patella. It cushions these bones and provides a smooth bearing surface so that bones glide easily past each other during knee motion.

Articular cartilage is comprised of chondrocytes (5% v/v) and an extracellular matrix (95% v/v). The later contains water (75% v/v), collagen (mainly type II) (20%), proteoglycans (5%), enzymes, growth factors (PDGF, TGF-beta, FGF, IGF-1), lipids and adhesives (fibronectin, chondronectin). Chondroblasts are the differentiation products of mesenchymal stem cells, which upon maturation are called chondrocytes. Chondrocytes, the only cell type in cartilage, maintain articular cartilage through production of collagen, proteoglycans and enzymes for cartilage metabolism.

Collagen provides the structural form and strength to cartilage. A typical collagen molecule is a long, stiff, triple-stranded helical structure. Each α -helical chain contains repeating units of Glycine-X-Y amino acids, where X is commonly proline and Y is commonly hydroxyproline.

The collagen fibrils are embedded in a hydrophilic gel made of various polysaccharide polymer chains of the class called glycosaminoglycan (GAG). The most abundant GAGs found in articular cartilage include hyarulonic acid (hyaluronan),

dermatan sulfate, keratan sulfate, and chondroitin sulfate. Except hyaluronan, these GAG molecules are usually found covalently linked to a protein, forming a large aggregated macromolecule called proteoglycan (PG) monomer. The proteoglycan monomers are then attached to the hyaluronic acid chain to form an amorphous gel. The proteoglycan's high density of electronegative charges attracts cations that create a swelling pressure that then enables the matrix to withstand compressive forces.

Water makes up 75% of the wet weight of the extracellular matrix of cartilage. It allows deformation of the surface by shifting in and out of the proteoglycan matrix during stress. Increased water content causes an increase in the permeability, decreased strength and decreased Young's modulus i.e. less stiffness.

Articular cartilage has four distinct zones (Fig. 1.1). From surface to deep they are identified as superficial tangential zone, transitional or middle zone, radial or deep zone and calcified zone. Each of the four zones has specific chondrocyte morphology and collagen distribution which helps each zone to play a specific role in resisting particular mechanical forces.

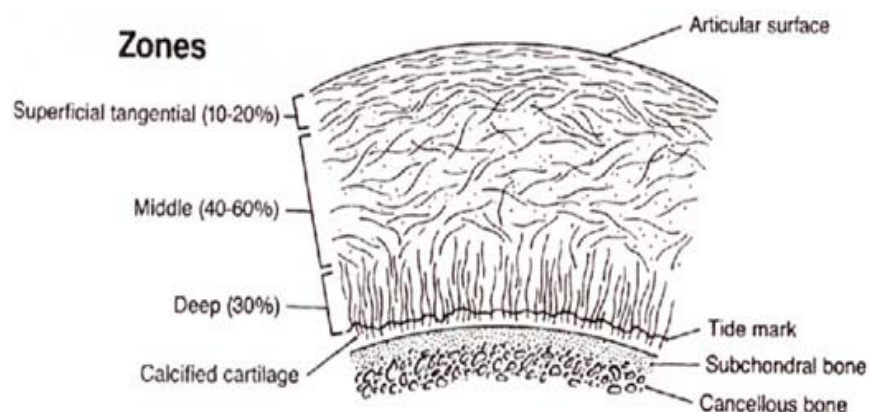


Figure 1.1 Four zones of articular cartilage. (Mow et al., 1992)

Biomechanics of articular cartilage

Articular cartilage is a biphasic material: a mixture of a porous, permeable viscoelastic solid (proteoglycan, collagen) and a moveable interstitial fluid (water and dissolved ions). Both phases are assumed to be intrinsically incompressible, and diffusive drag forces between the two phases give rise to the viscoelastic behavior of the tissue (Mow et al., 1980). It exhibits linearly elastic behavior at relatively low stresses and undergoes plastic deformation at high stress levels. Under constant magnitude load, the cartilage initially responds with a relatively large elastic deformation. The applied load extrudes water out of the cartilage matrix due to a load-induced pressure gradient and makes the matrix stiffer due to compaction of collagen fibers. As the load is maintained, the amount of deformation increases at a decreasing rate. After removal of load there is an instantaneous elastic recovery, due to water rushing into the matrix, followed by a more gradual creep-recovery. In contrast to bone, articular cartilage tends to stiffen with increasing strain.

Because of the low permeability of cartilage matrix, the fluid pressure inside the cartilage can rise to very high levels. The physiological levels can vary between 3 to 13 MPa [Mow et al., 1992]. The intermittent hydrostatic pressure has been shown to induce chondrogenic differentiation and cartilaginous matrix production in many studies [Elder et al., 2000; Parkkinen et al., 1993; Angele et al., 2003].

Using finite element computer analysis, Carter and Wong (2003) have theoretically concluded the role of local tissue mechanics in articular cartilage and tested the conclusions against *in-vitro* cell and tissue and molecular biology experiments. The

local intermittent hydrostatic pressures have been shown to promote cartilage maintenance in all the four zones of cartilage by maintaining chondrocyte phenotype and regulating cartilaginous matrix production. Cartilage explant, chondrocyte monolayer and three-dimensional chondrocyte culture studies indicate that mechanical forces of compressive, hydrostatic and/or fluid shear nature at frequencies ranging from 0.01 Hz to 1 Hz and the duration of applied force are critical parameters that stimulate the synthesis of the cartilage extracellular matrix, matrix proteins and may even enhance the mechanical properties of the developing tissue (Sah et al., 1989; Kim et al., 1994; Parkkinen et al., 1993; Jin et al., 2001; Smith et al., 1995; Elder et al., 2000; Elder et al., 2001; Smith et al., 1996; Carver and Heath, 1999; Vunjak-Novakovic et al., 1999).


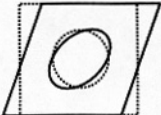
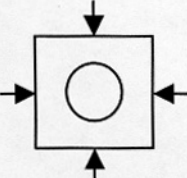

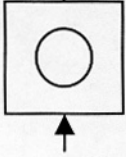

Test Condition	Cell/Matrix Deformation	Strain Components
Simple Shear 		Distortional Only
Hydrostatic Compression 		Volumetric Only
Unconfined Compression 		Distortional + Volumetric (+ Fluid Flow)

Figure 1.2 Strains produced in various loading conditions.

Hydrostatic pressure can be defined as the pressure exerted or transmitted by liquid (generally water) at rest. The pressure at a given depth in liquid is independent of direction and is the same in all directions. In other words, hydrostatic pressure has no direction associated with it when it is not in contact with some surface; however, the pressure on a submerged object is always perpendicular to the surface at each point on the surface. As compared to other type of forces, the hydrostatic pressure is characterized by only volumetric changes in a submerged object (Fig 1.2).

Hydrostatic pressure is indicated to play an important role in cell differentiation. Angele et al. (2003) have demonstrated that cyclic hydrostatic pressure enhances the chondrogenic phenotype of human mesenchymal progenitor cells differentiated *in-vitro*.

Cell Differentiation and Chondrogenesis

Mesenchymal stem cells (MSC) are nonhematopoietic pluripotent progenitor cells found within the bone marrow stroma. These cells have the potential to become tissue specific cells, the process of which is called differentiation. MSC can be differentiated *in-vitro* or *in-vivo* to terminally differentiate into osteoblasts, chondrocytes, adipocytes, tenocytes, myotubes, neural cells and hematopoietic-supporting stroma (Fig. 1.3).

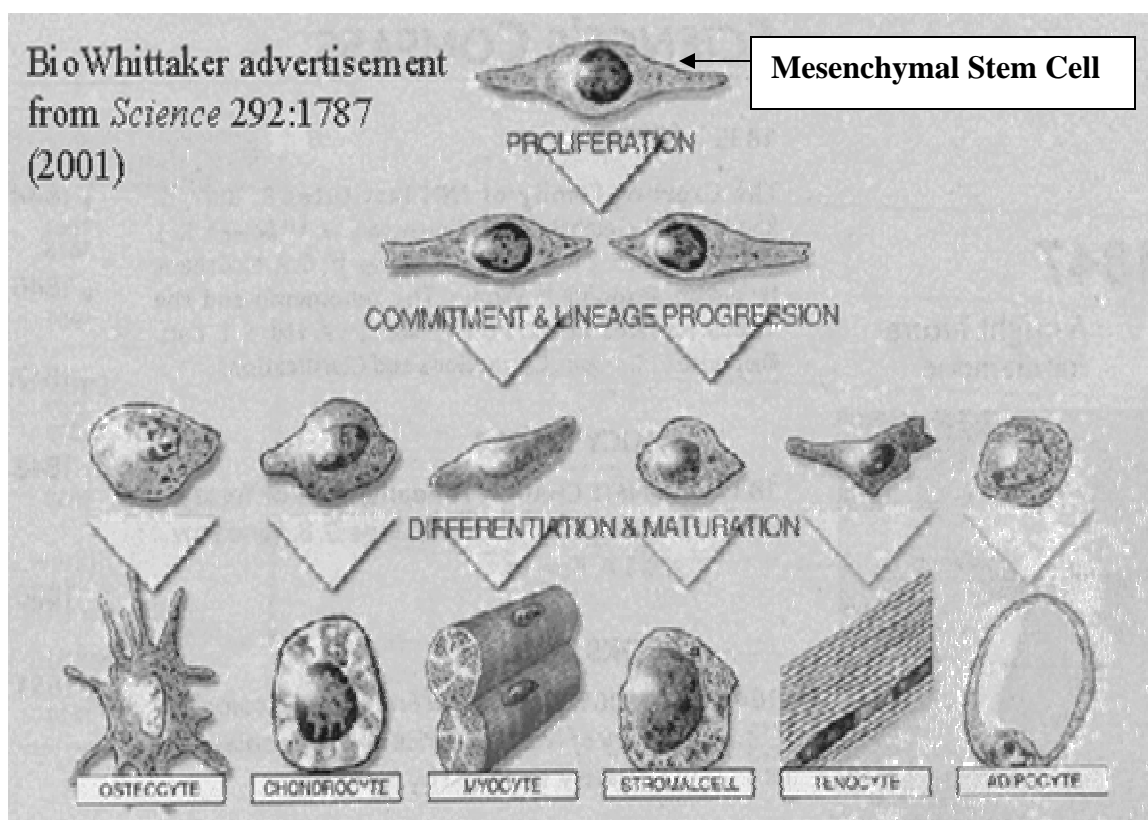


Figure.1.3 Mesenchymal Stem Cell Differentiation: Steps and Terminal Cell Types.

The multi-lineage potential of these cells, their easy isolation and culture, as well as their high *ex-vivo* expansive potential make these cells an attractive therapeutic tool. The cultures of MSC are not homogeneous but consist of an assortment of uncommitted and committed progenitors exhibiting divergent stemness. As progenitors progress towards the terminal phenotype, self-renewal is gradually lost and commitment increases. The terminal commitment of MSC is dependent on the microenvironment and biochemical stimuli. MSC differentiation to three tissue specific cell types is discussed below in terms of stimuli and identification markers.

Differentiation To:	Stimuli	Terminal Phenotype Identification Markers	
		Molecular	Cellular
Adipocytes	Dexamethason + insulin Dexamethasone + isobutylmethylxanthine	PPAR γ 2, C/EBP β , aP2, Adipsin, Leptin, Lipoprotein lipase	Cytoplasmic lipid droplet accumulation
Chondrocytes	TGF β 3 + ascorbic acid TGF β 1 + ascorbic acid	Cbfa-1, Collagen types II and IX, Aggrecan	Matrix enriched in proteoglycans and collagen types II and IX
Osteoblasts	Dexamethasone + β -glycerophosphate + ascorbic acid	Cbfa-1, Bone/liver/kidney alkaline phosphatase, Bone sialoprotein, Osteopontin, Osteocalcin, Collagen type I and II, Proteoglycans	Mineralized matrix formation

Table 1.1 Differentiation Potential of Bone Marrow-Derived Mesenchymal Progenitors *in-vitro*: Stimuli, Molecular and Cellular Markers (Minguell et al., 2001)

The chondrogenic potential of MSC has been demonstrated *in-vitro* by compressive loading (Elder et al., 2000) and by osteoinductive-proteins stimulation (Atkinson et al., 1997). During embryonic development, mesenchymal cell condensation provides the physical and biochemical environment factors conducive for cartilage formation. In articular cartilage, chondrogenesis is a multistep pathway that involves cell-cell communication induced differentiation of mesenchymal stem cells, followed by expression of cartilage-specific genes producing extracellular matrix proteins and mechanical stimulation induced maturation of prechondrocytic cells into mature chondrocytes specific to the four zones.

Murine fibroblast C3H10T1/2 cells have potential to differentiate into myoblasts, osteoblasts, adipocytes and chondrocytes through treatment with mutagenizing agents or bone-derived growth factors. C3H10T1/2 cells are an attractive system for the study of chondrogenesis because they represent a homogeneous population of multipotential cells that do not spontaneously differentiate under normal culture conditions (Denker et al., 1999). While previous C3H10T1/2 differentiation studies observed few chondrocytes compared to the other differentiated cell types, Denker et al. (1999) succeeded in enhancing chondrogenesis in C3H10T1/2 cells, with few other cell types present, by means of high-density micromass culture and BMP-2 treatment.

Principles of Cell Mechanics for Cartilage Tissue Engineering

The factors that influence the cartilage regeneration are cell-cell communication, cell-matrix interaction, growth factors and physical stimulation. Engineered tissue constructs implanted in the body are subjected to a complex biomechanical environment, potentially consisting of time-varying changes in stresses, strains, fluid pressure, fluid flow, and cellular deformation (Frank and Grodzinsky, 1987; Lai et al., 1991; Guilak et al., 1995). There is ample evidence for the importance of mechanical forces in facilitating articular cartilage regeneration (reviewed in Shieh and Athanasiou, 2003). Therefore mechanical forces may play an important role in the eventual success or failure of engineered cartilage. While these evidences hold great promise in tissue engineering, there is still no widespread agreement on the exact type and magnitudes of mechanical signals that are most crucial to cell function modulation.

Mechanisms for Mechanotransduction

The mechanical forces on cartilage and chondrocytes precipitate a host of biochemical changes in the cells and in the matrix environment around cells, which in turn can change the mechanical behavior of the tissue. While the influence of mechanical forces is well documented, the mechanism by which these cells interpret these forces and produce effective responses remains poorly understood. The main mechanisms proposed are physiochemical effects, ion pumps and channels, integrin signaling, cytoskeleton and nuclear deformation. Physiochemical effects like hypoosmotic stress, matrix fixed-charge density, interstitial ion concentrations, electrical potential, interstitial fluid flow and decreased pH are some of the effects generated during cartilage loading (Gray et al., 1988; Guilak et al., 2002; Kim et al., 1995). These physiochemical changes help cells understand mechanical load by inducing biochemical environmental changes that cells can understand, e.g. interstitial fluid flow.

Ion pumps and channels are common cellular signal transduction pathways. Hydrostatic pressure inhibits the Na^+/K^+ pump (ouabain-sensitive), $\text{Na}^+/\text{K}^+/\text{2Cl}^-$ cotransporter (bumetanide-sensitive), and residual (ouabain- and bumetanide-insensitive) pathways; however, the extent of inhibition of each system is dependent on pressure level and duration (Hall, 1999).

Integrins are the primary bridge between the extracellular matrix and the actin cytoskeleton and therefore are widely recognized as an important mechanotransduction element. Salter et al. (2001) has reviewed $\alpha 5\beta 1$ integrin as a mechanoreceptor in human articular chondrocytes. In brief, after stimulation of this integrin by mechanical

stimulation, there is activation of a signal cascade, involving stretch-activated ion channels, the actin cytoskeleton and tyrosine phosphorylation of the focal adhesion complex molecules. Subsequently, there is secretion of interleukin-4 (IL-4), which acts in an autocrine manner via Type II receptors, to induce membrane hyperpolarization. The IL-4 downstream signaling cascade and cell response may include increased aggrecan mRNA expression and decreased matrix metalloproteinase-3 mRNA expression. Abnormalities of chondroprotective mechanotransduction pathways in osteoarthritis may contribute to disease progression.

The cell nucleus is a viscoelastic solid material similar to the cytoplasm, but 3-4 times stiffer than and nearly twice as viscous as the cytoplasm (Guilak et al., 2000). Mechanical stress may influence gene expression through a direct physical connection from the extracellular matrix across the plasma membrane and to the nucleus. Buschmann et al. (1996) noted that the aggrecan synthesis correlates with cell and nucleus structure in statically compressed cartilage; thereby indicating a role of the nucleus in intracellular mechanotransduction pathways.

Role of Cytoskeleton

All of above proposed mechanisms involve the cytoskeleton directly or indirectly in mechanotransduction pathways. Therefore, the cytoskeleton is considered as a potential force transducer in cells (Durrant et al., 1999; Idowu et al., 2000; Jortikka et al., 2000; Langelier et al., 2000; Lee et al., 2000). Because of its structural role in the cell, the cytoskeleton can undergo numerous changes under load, including deformation,

reorganization, assembly and disassembly. The goal of this research is to determine the importance of the cytoskeleton in the transduction of mechanical signals by mesenchymal stem cells.

The cytoskeleton is composed of microfilaments, microtubules, and intermediate filaments (microtubules shown in Fig.1.4). These dynamic structures which extend throughout the cytoplasm, give cells the ability to adopt a variety of shapes, to coordinate and direct movements. It also facilitates intracellular transport of organelles and proteins, and segregation of chromosomes at mitosis. Each type of filament is a polymer product made of different protein monomers: actin for microfilament, tubulin for microtubules, and a family of related fibrous proteins, such as vimentin or lamin for intermediate filaments.

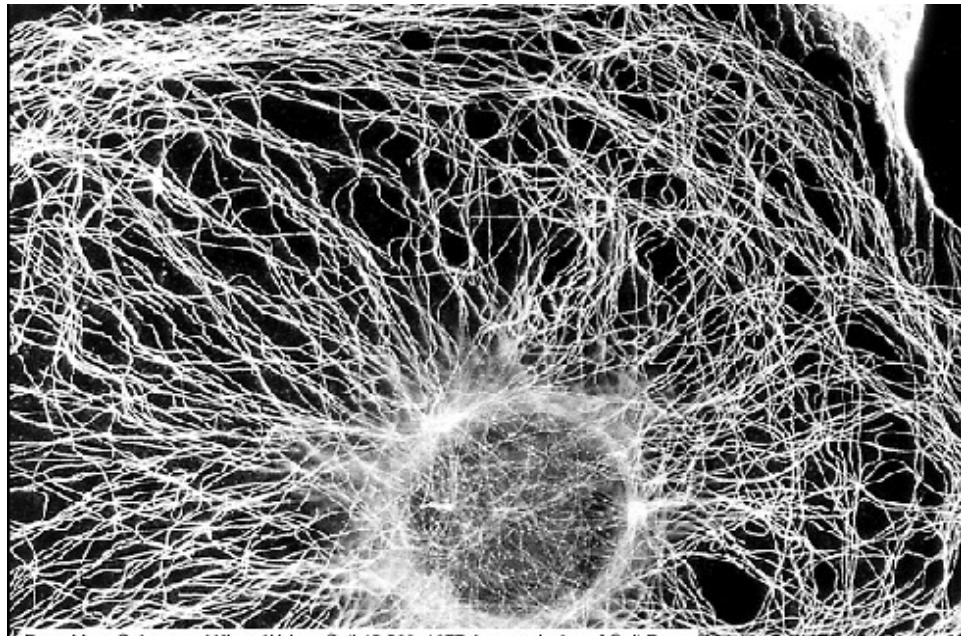


Figure 1.4 Microtubule structure in transformed cells. (Osborn and Weber, 1977)

Microfilaments (also known as actin filaments), two-stranded helical polymers of the protein actin, are abundant in cells and constitute 5% of the protein composition of the cell. They appear as flexible structures, with a diameter of 5-9 nm, that are organized into a variety of linear bundles, two dimensional networks, and three-dimensional gels. Actin filaments are essential for many movements of the cell, and they can be arranged in stress fibers to give cells high tensile strength. Although actin filaments are dispersed throughout the cell, they are highly concentrated in the cortex, just beneath the plasma membrane. Actin cortex which lies just beneath the plasma membrane can be locally restructured by localized extracellular signals. In a reciprocal way the organization of the actin cortex can have a significant effect on the shape and behavior of the overlaying plasma membrane.

Microtubules are long, hollow cylinders made of the tubulin dimer with polymers of α -tubulin subunit containing GTP and β -tubulin subunit containing GDP. Because of GTP and GDP actin, the dimer is either in steady growth or rapid disassembly, called "dynamic instability". With an outer diameter of 25 nm, they are much more rigid than actin filaments. Microtubules are long and straight and typically have one end attached to a single microtubule organizing center (MTOC) called a centrosome. The shaping of the plasma membrane by underlying actin cortex can move the centrosome which can induce reorganization changes in microtubules thereby polarizing cell movement. Microtubules are thought to be primary organizers of the cytoskeleton. Actin and microtubule also help intracellular transport of organelles using motor proteins which bind to either of them and use the energy derived from repeated cycles of ATP hydrolysis to move along it.

Intermediate filaments are rope-like fibers with a diameter of around 10 nm. These polymeric structures are made of intermediate filament protein monomers which constitute a large and heterogeneous family. One type of intermediate filament forms a meshwork called the nuclear lamina just beneath the inner nuclear membrane. Other types extend across the cytoplasm, giving cells mechanical strength and carrying the mechanical stresses in an epithelial tissue by spanning the cytoplasm from one cell-cell junction to another.

Mechanotransduction and cytoskeleton

The levels of microfilaments, microtubules and intermediate filaments vary from zone to zone in cartilage, which may be correlated to the different load environments in each zone (Idowu et al., 2000; Langelier et al., 2000). As described earlier, the mechanical signals stimulate the synthesis of extracellular matrix (ECM) proteins and alter gene expression, often in an ECM-dependent manner (Kim et al., 1999). ECM itself can regulate integrin-mediated signaling events that control growth, differentiation, motility, apoptosis and matrix synthesis and remodeling (Boudreau and Bissell, 1998). The cell cytoskeleton elements are coupled to extracellular matrix (ECM) through cell surface receptors and therefore are a potent candidate for the mechanism of mechanotransduction. Specifically, integrins interact with ECM components via their extracellular domains, while their cytoplasmic domains interact with the cytoskeleton, signaling molecules and other cellular proteins, resulting in regulation of many biological functions.

Tensegrity model (Ingber, 1997) predicts that cells are hard-wired to respond immediately to mechanical stresses transmitted over cell surface receptors that physically couple the cytoskeleton to extracellular matrix, or in other words, cells exist in an equilibrium balance of forces. Therefore applied mechanical signals that affects ECM mechanics, can directly induce changes in this preexisting cellular force balance, resulting in alternations in the mechanics of the cytoskeleton. Mechanical tension generated within the cytoskeleton can be a critical regulator of cellular functions ranging from the control of chromosome movement to the gene expression (Chicurel et al., 1998). Mechanical stress and strain have been shown to affect the cytoskeleton structure and response (Wang et al., 1993; Meazzini et al., 1998), suggesting the involvement of cytoskeleton in mechanotransduction.

Chicurel et al. (1998) predicted the possibility of altering microtubule (MT) assembly by applying compressive forces using the tensegrity model. The theory has been tested true by Putnam et al. (2001) by applying mechanical strain and by changing the density of ECM ligand used for cell adhesion. It was found that a positive 10% step change in the substrate strain increased MT mass by 34% over static control and a negative 10% step change in strain decreased MT mass by 40%. Jortikka et al. (2000) have shown that stimulation of proteoglycan synthesis by cyclic hydrostatic pressure does not occur if the dynamic nature of MTs is disrupted by the microtubule disrupting drug Nocodazole. Similarly, Tumminia et al. (1998) have shown that mechanical stretch alters the actin cytoskeletal network. Zanetti and Solursh (1984) have shown that actin disruption can induce chondrogenic differentiation of mesenchymal stem cells.

Tools for Cytoskeleton Study

Cytoskeleton disruption is an effective tool to study the cytoskeleton mediated signal transduction pathways. For example, using microtubule disruption drugs, Jortikka et al. (2000) found that in a monolayer chondrocyte culture, inhibition of proteoglycan synthesis by continuous high hydrostatic pressure does not interfere with the microtubule-dependent vesicle traffic, while the stimulation of proteoglycan synthesis by cyclic pressure does not occur if the dynamic nature of microtubules is disrupted.

Cytochalasins are a group of related fungal metabolites, all characterized by a highly substituted hydrogenated isoindole ring to which is fused a macrocyclic ring. Cytochalasin B (molecular formula: $C_{29}H_{37}NO_5$) and Cytochalasin D (molecular formula: $C_{30}H_{37}NO_6$) have the capacity to disrupt microfilaments. These cytochalasins are cell membrane permeable and inhibit cell division by blocking formation of contractile microfilaments. They also inhibit cell movement, induce nuclear extrusion, and shorten actin filaments by blocking monomer addition at the fast growing end of the polymer. However, Cytochalasin B also inhibits glucose transport which might not be desirable for some studies. Cytochalasin D possesses antibiotic and antitumor activity and is also implicated in promoting conditions favorable for depolymerizing actin.

Another important tool for cytoskeleton studies is indirect immunofluorescence confocal microscopy. The normal steps in the process include chemical fixation, membrane permeabilisation, blocking non-specific antibody binding, tagging cytoskeletal elements under investigation with a specific primary antibody and then adding a FITC labeled secondary antibody which binds to the primary antibody. FITC labeled antibodies

have specific excitation and emission wavelength which can be used in confocal microscopy to view the cytoskeletal elements tagged by the primary antibody.

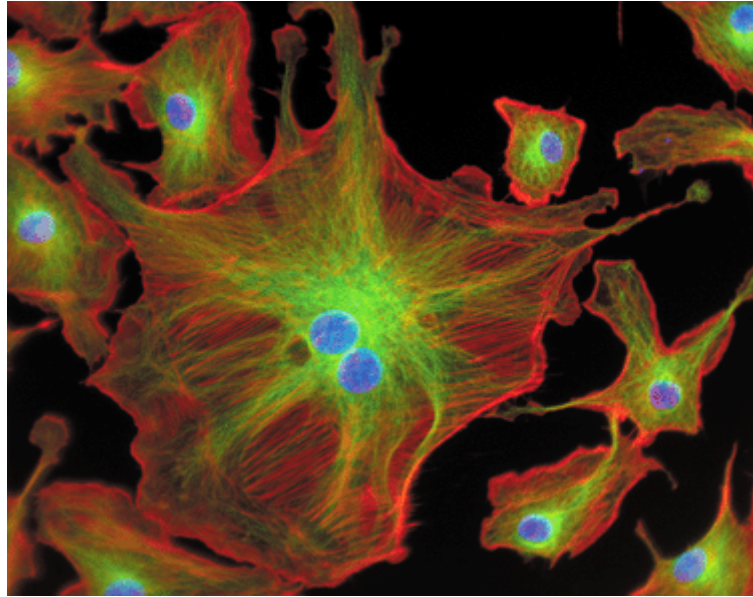


Figure 1.5 Actin (red) and microtubule (green) structures shown in cow endothelial cells. The nucleus is stained blue. (Molecular Probes®)

Gene Expression and Growth Factors

Chondrogenesis is regulated by a complex interaction between genetic and epigenetic factors. Mechanotransduction occurs through the extracellular matrices, modifying cell–matrix and cell–cell interactions, and impacting on transcriptional factors. The gene expression in chondrocytes is altered by tensile and compressive forces (Takahashi et al., 1998 and 2003), cell-cell communication, cytoskeleton, extracellular matrix and growth factors. A number of molecules have been shown to function in

cartilage formation. These include classes of extracellular ligands and their cognate receptors and cytoplasmic transducers, nuclear receptors, transcription factors or DNA-binding proteins, matrix proteins, matrix metalloproteinases, adhesion molecules and the cytoskeleton. The interplay, therefore, between genetic and biomechanical determinants controls the integrity of cartilage produced *in-vivo* and *in-vitro*.

Cell-cell and cell-matrix interactions activate cytoplasmic kinases, phosphatases and GTPases that can, in turn, be modulated by signaling from growth and differentiation factors such as the bone morphogenetic proteins (BMPs) (Haas and Tuan, 1999). BMP, a subgroup of its superfamily transforming growth factor (TGF- β), members of which have been strongly implicated in skeletal development. The TGF- β 1, TGF- β 2, TGF- β 3 and BMP-2 promote the chondrogenic differentiation of mesenchymal cells in high density micromass cultures (Denker et al., 1999; Roark and Greer, 1994). However, TGF- β appears to be most effective on cells which have not yet undergone cell condensation, a critical event in early cartilage differentiation, whereas BMP-2 is most effective after cells have condensed or differentiated. This indicates that TGF- β and BMP-2 act in a sequential manner to regulate mesenchymal cells through the different stages of chondrocyte differentiation, its mechanical regulation and cartilage formation.

Conversely, different types of mechanical forces have the ability to regulate TGF- β and BMP mRNA expression. Mechanical tension-stress has been shown to induce expression of BMP-2 and BMP-4 during distraction osteogenesis (Sato et al., 1999). Similarly cyclic hydrostatic pressurization of chondrosarcoma cells have shown to up-regulate and down-regulate many gene expressions (Karjalainen et al., 2003).

Statement of Hypothesis

This research focuses on role of actin cytoskeleton filaments (microfilaments) in mediating the response of chondroprogenitor cells to cyclic hydrostatic pressure. To test this hypothesis, multipotential murine fibroblast mesenchymal C3H10T1/2 cells are subjected to hydrostatic pressure to induce chondrogenic differentiation. In the chondroinductive pressurization system, the actin cytoskeleton filaments will be disrupted using actin disrupting drug Cytochalasin D and the chondrogenic effect is reassessed.

Objective

To determine the role of actin cytoskeleton filaments (microfilament) in mediating the response of chondroprogenitor cells to cyclic hydrostatic pressure.

Specific Aims:

1. Evaluate cytotoxicity and determine working concentration of Cytochalasin D for actin disruption in C3H10T1/2 cells.
2. Determine whether specific cytoskeleton elements are involved in cell shape changes correlated with enhanced chondrogenesis.
3. Develop and characterize a hydrostatic pressurization system to induce chondrogenesis in C3H10T1/2 cells.
4. In chondroinductive pressurization system, disrupt the actin cytoskeleton filaments and reassess chondrogenic effect of cyclic hydrostatic pressurization.

CHAPTER II

METHODS AND MATERIALS

Experimental Design Outline

Murine C3H10T1/2 cells of fibroblastic morphology are used in this study since they represent a homogeneous population of multipotential cells that do not spontaneously differentiate under normal culture conditions (Denker et al., 1999). Successful disruption and immunofluorochemical visualization of actin cytoskeleton elements is critical to address all the specific aims. Therefore, first, the actin elements in pluripotential C3H10T1/2 cells were studied using immunofluorescence techniques. Actin fibers were stained with a fluorescent and biotinylated phallotoxin that specifically stains polymeric actin filaments (F-actin). The phallotoxins which are isolated from the deadly *Amanita phalloides* mushroom are extremely water soluble, thus providing convenient probes for labeling, identifying and quantitating F-actin in tissue sections, cell cultures or cell-free experiments. Unlike antibodies, phallotoxins have similar affinity for both large and small filaments, binding in a stoichiometric ratio of about one phallotoxin molecule per actin subunit. Nonspecific staining is negligible, and the contrast between stained and unstained areas is extremely large.

For comparison purposes, the tubulin filaments were also visualized. Tubulin fibers were visualized via indirect immunostaining technique. Fluorescein isothiocyanate

(FITC) conjugated goat anti-mouse secondary antibody was bound to monoclonal anti- α -tubulin primary antibody attached to tubulin. A Leica TCSNT Confocal Laser Scanning Microscope was used for imaging the cytoskeletal elements.

Figure 2.1 shows the experimental design flow diagram to address specific aims.

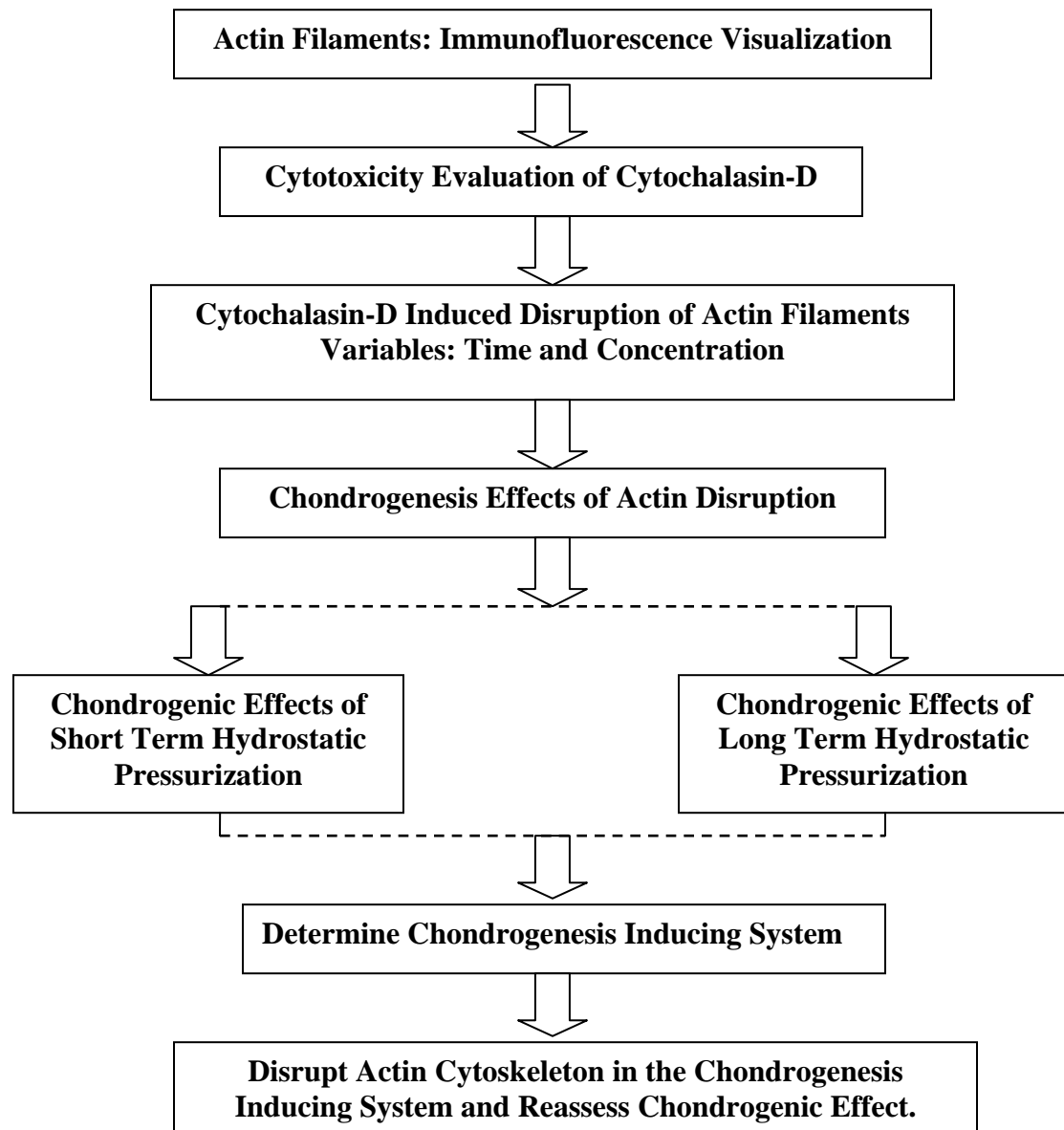


Figure 2.1 Experimental design flow-diagram.

Specific Aim 1: The cytotoxic effects of the actin disrupting drug Cytochalasin-D was assessed on pluripotential C3H10T1/2 cells using the CellTiter 96[®] AQueous One Solution Cell Proliferation Assay (Promega Corp; Madison, WI). The CellTiter 96[®] AQueous One Solution Reagent contains a tetrazolium compound [3-(4,5-dimethylthiazol-2-yl)-5-(3-carboxymethoxyphenyl)-2-(4-sulfophenyl)-2H-tetrazolium, inner salt; MTS^(a)] and an electron coupling reagent (phenazine ethosulfate; PES). MTS is bio-reduced by cells into a formazan product that is soluble in tissue culture medium. The absorbance of the formazan at 490 nm can be measured directly using a spectrophotometer without additional processing.

The pluripotential C3H10T1/2 cells were cultured on glass coverslips. Varying concentrations of Cytochalasin D were added to disrupt actin filaments. The cells were exposed to the drug for variable time durations. The depolymerization of actin fibers was visualized by immunofluorescence-confocal microscopy techniques. The final concentration of the drugs to be used was determined as that which achieved >90% disruption of the cytoskeletal elements. The minimum time required to achieve this disruption was determined. Also, cell viability and effect on the actin filaments after removal of drug were assessed. The actin cytoskeletal elements were found to reorganize themselves after removal of the drug. The time required for reorganization was determined.

Specific Aim 2: This specific aim examined if the disruption of the actin cytoskeletal elements alone can induce chondrogenic differentiation in pluripotent C3H10T1/2 cells which have ability to differentiate into myoblasts, osteoblasts,

adipocytes and chondrocytes. The chondrogenesis was compared with proven BMP-2 induced chondrogenesis (Denker et al., 1999). C3H10T1/2 cells were cultured in high-density micromass or spot cultures and allowed to grow for 24 hours from the time of seeding. The cells were exposed to Cytochalasin-D for the next 24 hrs. Chondrogenesis was assayed by measuring sulfated glycosaminoglycan (sGAG) content qualitatively by Blyscan™ Glycoaminoglycan Assay (Biocolor, Northern Ireland, UK) and quantitatively by Toluidine Blue staining. Actin disruption was checked by immunofluorescence, and cell proliferation was assessed by DNA quantification.

Specific Aim 3: The effect of hydrostatic pressurization on chondrogenesis in C3H10T1/2 cells was studied for short and long term pressurization. Chondrogenesis was evaluated based on DNA content, total sulfated glycosaminoglycan (sGAG) content, rate of total collagen synthesis (as indicated by macromolecular incorporation of [³H]Proline), and immunostaining (with a monoclonal antibody specific to type II collagen). The hydrostatic pressurization system that induces chondrogenesis was determined from short and long duration pressurization models.

Specific Aim 4: In the proven chondroinductive system, the cells were exposed to Cytochalasin D during hydrostatic pressurization to disrupt the actin cytoskeletal elements. Chondrogenesis was reassessed in this drug treated chondroinductive hydrostatic pressurization system. The presence or absence of chondroinductive effect in this system will indicate the role of actin cytoskeletal elements in chondroinduction by hydrostatic pressure.

Materials and Methods

Chemicals

BMP-2: Human recombinant BMP-2 was generously donated by Wyeth Inc. (Madison, NJ) or was purchased from R&D Systems Inc. (Minneapolis, MN). A concentrated stock was diluted in complete medium to obtain a working concentration of 100 ng/ml. BMP-2 was added to micromass culture when they were flooded with medium and then at every medium change.

Cytochalasin-D: Cytochalasin D was obtained from Sigma Chemical Co. (St. Louis, MO). The powder was dissolved in dimethylsulfoxide at a concentration of 1mg/ml, and then was diluted with tissue culture grade water to give final molarity of 200 μ M. The stock solution was diluted 1:50 in culture medium for routine use at 4 μ M/ml concentration unless otherwise mentioned. The final concentration of dimethylsulfoxide was 0.2% which is known to have no apparent effect on cell survival or differentiation.

Cell Culture

C3H/10T1/2

C3H/10T1/2 mouse embryo fibroblasts clone 8 cells (CCL-226, American Type Culture Collection, Manassas, VA) were maintained in monolayer cultures in standard 75-cm² (T-75) polystyrene tissue culture flasks (Corning Inc. NY). The cells were maintained in 1:1 composition of Dulbecco's Modified Eagle Medium (DMEM) and

Nutrient Mixture F-12 HAM (both, Sigma Chemicals Co., St. Louis, MO) supplemented with 10% heat-inactivated fetal bovine serum (FBS) (ATCC), and antibiotic antimycotic solution (100 units/ml penicillin G, 0.1 mg/ml streptomycin sulfate and 0.25 µg/ml amphotericin B). The same composition of complete medium was used for all experiments unless otherwise mentioned. For sub-culturing, subconfluent cells in the flasks were washed with Phosphate Buffer Saline (PBS) and trypsinized using 0.25% trypsin in PBS for several minutes. The detached cells, suspended in trypsin, were transferred to a centrifuge tube and bovine serum was added to deactivate trypsin. The cells were centrifuged and the formed pellet was resuspended in a small volume of complete culture medium. The cells were counted using a hemocytometer, and new flasks were seeded at 2000 viable cells per square centimeter of a culturing flask. All cultures were maintained in a 37°C incubator with a humidified atmosphere of 95% air and 5% CO₂.

For Study of Cytoskeletal Elements

C3H10T1/2 cells were cultured on 22 mm X 22 mm, No. 1 glass coverslips (Fisher Scientific, Pittsburg, PA). The coverslips were sterilized by dipping in 100% ethanol and flaming immediately. The coverslips were then preincubated with FBS, for better cell attachment, placed in wells of 6-well tissue culture plates and allowed to air dry. C3H10T1/2 cells grown in T-75 flasks were trypsinized, centrifuged and the pellet was resuspended in 0.5 ml of culture medium. The cell number was counted and 50 µl of

this 1.2×10^6 cells/ml suspension was placed at the center of each coverslip. The cells were allowed to adhere in incubator for 3 hours and then 3 ml of culture medium was added to each well. After 3 days, the cells were washed with PBS and processed for immunofluorescence study of actin filaments (using phalloidin) and tubulin filaments (using anti- α -tubulin primary antibody and FITC Conjugated goat anti-mouse antibody).

For Cytotoxicity Studies

For the standard curve in the proliferation assay, 4000, 8000, 16000, 32000 and 64000 C3H10T1/2 cells in 100 μ l of medium were cultured in a 96-well plate. The cells were allowed to adhere for 1 hour and then 20 μ l of tetrazolium compound solution from CellTiter 96[®] AQueous One Solution Cell Proliferation Assay (Promega Corp; Madison, WI) was added. The 96-well plate was incubated for 4 hours, and the absorbance was read at 490nm. For cytotoxicity studies, 25000 C3H10T1/2 cells were cultured in 96-well tissue culture plates. Varying concentrations of Cytochalasin-D (1, 2, 3, 4, 5, 10, 15, and 20 μ M) were added to independent wells for 2 hours, and the drug was removed by washing the cells two times with PBS. The cells were then cultured in the drug-free cell culture medium. The treatment with Cytochalasin D was repeated for 3 consecutive days. On the fourth day, the cytotoxicity of the drug to C3H10T1/2 cells was evaluated using CellTiter 96[®] AQueous One Solution Cell Proliferation Assay as described above.

For Actin Disruption Studies

C3H10T1/2 cells were cultured on coverslips as mentioned above. After 48 hours of incubation, the cells were exposed to 2 μM , 4 μM and 8 μM of Cytochalasin-D for 2 hours. The cells without any drug treatment were used as control. The cells were washed twice with PBS to remove the drug and processed for immunofluorescence study of actin filaments (using phalloidin). To investigate whether or not the effects of Cytochalasin D were reversible, the cells were treated as above and allowed to grow for 24 hours after removal of the drug in the drug free complete medium.

For Actin Disruption Induced Chondrogenesis Studies

C3H10T1/2 cells between the 5th and 15th passage were trypsinized and resuspended in the complete medium. For immunofluorescence studies, a 10 μl drop of this 5.6×10^6 cells/ml suspension was placed in the center of a glass coverslip that comprised the bottom of a chamber slide. The cells were allowed to adhere for 2-3 hours in an incubator and then 1 ml of medium was added. The cells were allowed to grow for 24 hours. The experimental cultures were treated with 4 μM Cytochalasin-D for next the 24 hours, and then incubated for an additional 24 hours in the absence of the drug. For a qualitative assessment of the chondroinductive influence of Cytochalasin-D on C3H10T1/2 cells, some cells were plated onto standard 24-well polystyrene tissue culture plates using the micromass technique described above. Cells were assigned to one of the 4 groups: control (no BMP-2 and Cytochalasin-D) (negative control), 100 ng/ml BMP-2 (positive control), 4 μM Cytochalasin-D or a combined treatment of 100ng/ml BMP-2

and 4 μ M Cytochalasin-D. The culture medium was changed every 3 days, and BMP-2 and Cytochalasin-D were replenished with each change. These cultures were examined only by Toluidine Blue staining for qualitative assessment of glycosaminoglycan as described later. For quantitative assessment of differentiation, cells were seeded into a 96-well, round bottom plate so as to promote more cell-cell interaction. Individual wells were assigned to the same four experimental groups. However, after 24 hours the cells were washed three times with fresh medium and cultured for an additional 10 days in the absence of any Cytochalasin-D. The culture medium was changed every 3 days, and BMP-2 was replenished with each change. On day 12, the DNA content was determined for cell proliferation, and total sulfated glycosaminoglycan content was determined as an indicator of chondrogenesis.

Chondrogenic Effect of Hydrostatic Pressurization

To study the chondrogenic effects of hydrostatic pressurization on C3H10T1/2 cells, the cells were seeded at a density of 7.5×10^4 cells/well into 3 \times 4-well sections cut from a round-bottom, 96-well plate. The chondroinduction medium was Dulbecco's Modified Eagle's Medium/Nutrient Mixture F-12 Ham (1:1) containing 10% fetal bovine serum, antibiotic antimycotic solution and 25 ng/ml recombinant human bone morphogenetic protein-2 (rhBMP-2). Four 3 \times 4-well sections were placed in separate flexible plastic bags that were filled with chondroinduction medium and heat-sealed.

Care was taken to remove all air bubbles since air is compressible and will cause non-uniform hydrostatic pressure in the liquid medium.

Two bags, designated as experimental, were pressurized, while the other two control bags were placed in the same assembly but were not subjected to any pressure. Experimental cultures were subjected to a 1.0 Hz sinusoidal hydrostatic compression waveform with a minimum applied pressure of 0.3 MPa and a maximum pressure of 5.0 MPa. Two pressurization time durations were chosen to see the effect of short and long duration pressurization on chondrogenesis. For short duration pressurization, the cells were pressurized during three 10-minute sessions, separated by 10-minute rest intervals, for a total of 1800 cycles per day on each of three consecutive days. For long duration pressurization, the cells were pressurized during twelve 10-minute sessions, separated by 10-minute rest intervals, for a total of 7200 cycles per day on each of three consecutive days. Immediately upon completion of loading, cultures were removed from the pressure vessel and returned to a water bath inside a standard tissue culture incubator (37°C, 95% air-5% CO₂). After 3 days of loading the plate sections were removed from the heat-sealed bags and maintained in static culture for the next 5 days. Ascorbic acid was added each day to a final concentration of 50 ng/ml.

At the end of 8 days, the chondrogenesis was assessed by qualitative and quantitative methods. Quantitative analysis of chondrogenesis was determined as sulfated glycosaminoglycan synthesis and rate of collagen synthesis while qualitative analysis was obtained as pericellular Alcian Blue staining for sulfated glycosaminoglycan and collagen

type II immunostaining. DNA content was quantified for each well and was used to normalize sulfated glycosaminoglycan synthesis for respective well.

A successful chondroinductive hydrostatic pressurization model was determined between the short and the long duration hydrostatic pressurization by quantitative and qualitative assessment of chondrogenesis.

Effect of Actin Disruption on Chondrogenesis by Hydrostatic Pressurization

In the chondroinductive hydrostatic pressurization model (short or long duration), the C3H10T1/2 cell actin cytoskeletal filaments were disrupted during the pressurization period using 2 μ M Cytochalasin D. Lower than normal concentration of the disruption drug was used to prevent the cells from completely detaching from the substrate. Even at 2 μ M concentration the drug is effective enough for 80% disruption of actin filaments as shown in the next chapter. Chondrogenesis was assessed again as above to determine existence of the same chondroinductive effect.

Pressurization System

Bags to be pressurized were placed within a custom device designed for the application of cyclic hydrostatic compression (Fig 2.2). The device consists of a large cylindrical stainless steel base connected to a lid by bolts that compress an intervening o-ring. A hydraulic cylinder is welded to the lid so that its interior is continuous with that

of the chamber. The cylinder and chamber are completely filled with water, so that rapid hydrostatic compression is achieved by a force (generated by a MTS servohydraulic testing machine) applied to the cylinder's piston. A stable 37° C is maintained by immersing the chamber in a temperature-regulated circulating water bath.

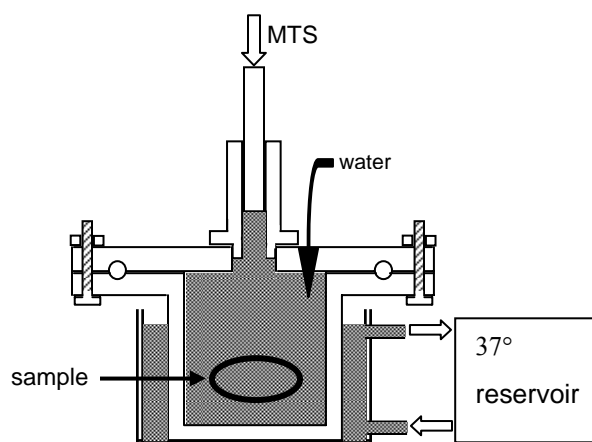


Figure 2.2 Schematic drawing of device for applying cyclic hydrostatic compression to cultured cells.

See Appendix A for working pictures of the hydrostatic pressurization device.

Immunofluorescence

Cells, whose actin cytoskeleton elements were to be studied, were cultured on chamber slides. Cultures to be stained for cytoskeletal elements were rinsed three times in phosphate buffer saline (PBS) and then permeabilized with 0.5% Triton X-100. Cultures were then again washed three times with PBS and fixed in 3% formaldehyde for 20 minutes. The cultures were then incubated for 30 minutes with 1% Bovine Serum Albumin (BSA) to avoid nonspecific staining. Actin cytoskeleton elements were stained

with Alexa Fluor 488 Phalloidin (Molecular Probes, Inc. Eugene, OR). The Phalloidin was dissolved in methanol to give stock solution concentration of 200 units/ml, which is approximately equivalent to 6.6 μ M. The Phalloidin was used after diluting 5 μ l of stock solution into 200 μ l of PBS for each slide. The Phalloidin staining solution was placed on the chamber slides for 20 minutes at room temperature. Cultures were washed three times with PBS and cover slips were placed over the cultures, with ProLong Antifade Kit (Molecular Probes) as the mounting medium. The Phalloidin was excited at wavelength of 495 nm and emission was captured at 518 nm on confocal microscope.

Tubulin cytoskeleton elements were tagged with a monoclonal anti- α -tubulin clone DM 1A antibody (Sigma Chemical Co) diluted 1:500. The primary antibody was placed on the chamber slides for 30 minutes and incubated at 37°C. The chamber slides were washed twice in PBS for 5 minutes. The tubulin fibers were then stained with FITC Conjugate Goat Anti-Mouse IgG (Sigma Chemicals Co.) that binds to the primary antibody and fluoresces green when excited at 488 nm. The secondary antibody was diluted 1:200 and was placed on chamber slides for 30 minutes at 37°C. The chamber slides were then washed twice with PBS for 5 minutes each. Cover slips were placed over the cultures, with ProLong Antifade Kit (Molecular Probes) as the mounting medium.

For convenience 1 μ g/ml propidium iodide was used to counterstrain the cell nuclei. Phalloidin and anti- α -tubulin antibody stained cultures were imaged on Leica TCSNT Confocal laser scanning microscope (Mississippi State University, Electron Microscopy Center).

Assessment of Chondrogenesis

DNA Quantification

For determination of DNA content, cells were lysed in 300 μ l of 0.5% v/v Nonidet P-40, 50 mM Tris-Cl, 100 mM NaCl, 5 mM MgCl₂. The lysate was transferred to microcentrifuge tubes, centrifuged at maximum speed for 5 minutes, and DNA in a 100 μ l of supernatant was measured using the Hoescht dye method (DNA Quantification Kit Fluorescence Assay, Sigma Chemicals Co.) with calf thymus DNA as a standard.

Sulfated Glycosaminoglycan Quantification

The remaining lysis buffer was removed and sGAG digested in 100 μ l of 2% v/v papain and L-Cystein in 50 mM sodium acetate (pH 6) overnight at 60°C. Total sGAG content was then measured by the dimethylmethylene blue precipitation method (BlyscanTM Glycoaminoglycan Assay, Biocolor, Northern Ireland, UK) using chondroitin 4-sulfate purified from bovine trachea as a standard. The cationic dye (1,9 dimethylmethylene blue) binds to proteoglycans and sulfated GAGs in the culture medium and forms a precipitate which was separated out by microcentrifugation. The precipitate was then dissolved in a dissociation reagent containing Propan-1-ol and Guandidine HCl. Color intensity, which is proportional to the amount of the GAG in sample, was measured at 656 nm using a μ Quant Universal Microplate Spectrophotometer (Bio-Tek Instruments, Winooski, VT). GAG concentration was

determined by using the standard curve equation. For each sample, sGAG content was normalized to DNA content.

Rate of Collagen Synthesis

In wells in which the rate of collagen production was to be determined, the medium was removed and replaced with serum-free Dulbeccos's modified Eagle medium containing [³H]proline at 10 μ Ci/ml, 25 μ g/ml ascorbic acid, an 100 μ g/ml β -amino-propionitrile (β -APN) to inhibit collagen cross-link formation. After a 24-h incubation period, incorporation of [³H]Proline into collagen was measured by the rapid filtration method of Koyano et al. [1997]. Briefly, the medium was removed and the cell layer was washed with PBS and extracted with 0.5 M acetic acid for 24 h at 4°C. Durapore membranes of a 96-well Filtration Plate (Millipore Multiscreen® Assay System, 0.65- μ m pore size), were soaked with 50 μ l of 25% trichloroacetic acid (TCA). Fifty microliters of the cell extract and 50 μ l of 50% TCA were then added to the Filtration Plate and the plate was incubated at 4 °C for 1 hour. The precipitate formed was collected on the filter membranes and separated from the supernatant using a vacuum manifold. After washing 3 times with 100 μ l of 10% TCA to remove unincorporated tracer, filter membranes were punched out into scintillation vials, and the filter-bound radioactivity was quantified by liquid scintillation counting.

Collagen Type II Immunostaining

The presence of cartilage-specific type II collagen was detected by immunostaining with the monoclonal II-II6B3 antibody (Developmental Studies Hybridoma Bank, University of Iowa, Iowa City, IA). Cultures were rinsed with PBS, fixed in 95% v/v methanol, 3% v/v glacial acetic acid and allowed to air dry overnight. They were then stained using a labeled-[strept]avidin-biotin technique [Histostain®-SP, Zymed Laboratories, South San Francisco, CA]. The specificity of the antibody binding was confirmed by substituting PBS for the primary antibody in control samples.

Alcian Blue and Toluidine Blue Staining

Alcian Blue (pH 2.5) was made by dissolving 1.0 g of Alcian Blue powder with 97 ml of water and 100 ml of glacial acetic acid. The samples to be stained were rinsed with PBS, and cells were fixed with 10% neutral buffer formalin for 20 minutes. The samples were stained with hemotoxylin for 3 minutes and washed with distilled water. The samples were then stained with Alcian Blue or Toluidine Blue for 30 minutes. The stained samples were destained with 0.5 M acetic acid, dehydrated in ethanol and allowed to air dry.

Statistics

All statistical analysis was performed using Statlets software (StatPoint LLC) which was downloaded from [<http://www.statlets.com>].

The cytotoxicity evaluation of Cytochalasin D was statistically analyzed using linear correlation. The correlation coefficient was determined and the P-value for the slope of the line was determined at the 95% confidence level ($\alpha = 0.05$).

In actin disruption effect on chondrogenesis experiment, the sulfated glycosaminoglycan normalized to DNA was statistically analyzed by two-way ANOVA at the 95% confidence level, and the interaction plot between BMP-2 and Cytochalasin D was plotted.

For evaluating the chondrogenic effects of hydrostatic pressurization, measurements of sulfated glycosaminoglycan were normalized to DNA and the rates of collagen synthesis were analyzed by the two-sample independent t-test at the 95% confidence level. Since the two independent sample t-test depends on equal or unequal variances, the F-test was performed. The F-test requires that the data is normally distributed; therefore, the data was checked for normal distribution by box-and-whisker plot and plotting histogram.

CHAPTER III

RESULTS

Actin filaments: Immunofluorescence Visualization

Primary antibodies specific to actin or tubulin filaments and fluorescein labeled secondary antibodies specific to primary antibodies were used to study respective filaments' normal distribution in C3H10T1/2 cells. The images were captured on a confocal microscope at 400 magnification (Fig. 3.1 A) and 630 magnification (Fig. 3.1 B). The actin filaments (fluorescing red) can be observed throughout the cytoplasm; however, they are more concentrated near the periphery of the cells. Some concentration points can be observed in the periphery of cells where many actin filaments seem to converge. These concentration points are believed to be point of contact with the substrate. The actin filaments of a cell are also observed to be uniting with the actin filaments of other cells. These observations suggest the role of actin filaments in cell-cell, cell matrix and cell-substrate communication.

The tubulin filaments (fluorescing green) can be observed as filaments radiating from the perinuclear to peripheral areas. They are more concentrated around cell nucleus, thereby supporting the nucleus. In each cell, a bright green spot, called the centrosome, can be observed around the cell nucleus (which is microtubule organizing center). The

lower cell in Fig. 3.1 B is undergoing cell division and the role of the centrosome in cell division is conclusive due to the brighter green spot around the dividing cell nucleus.

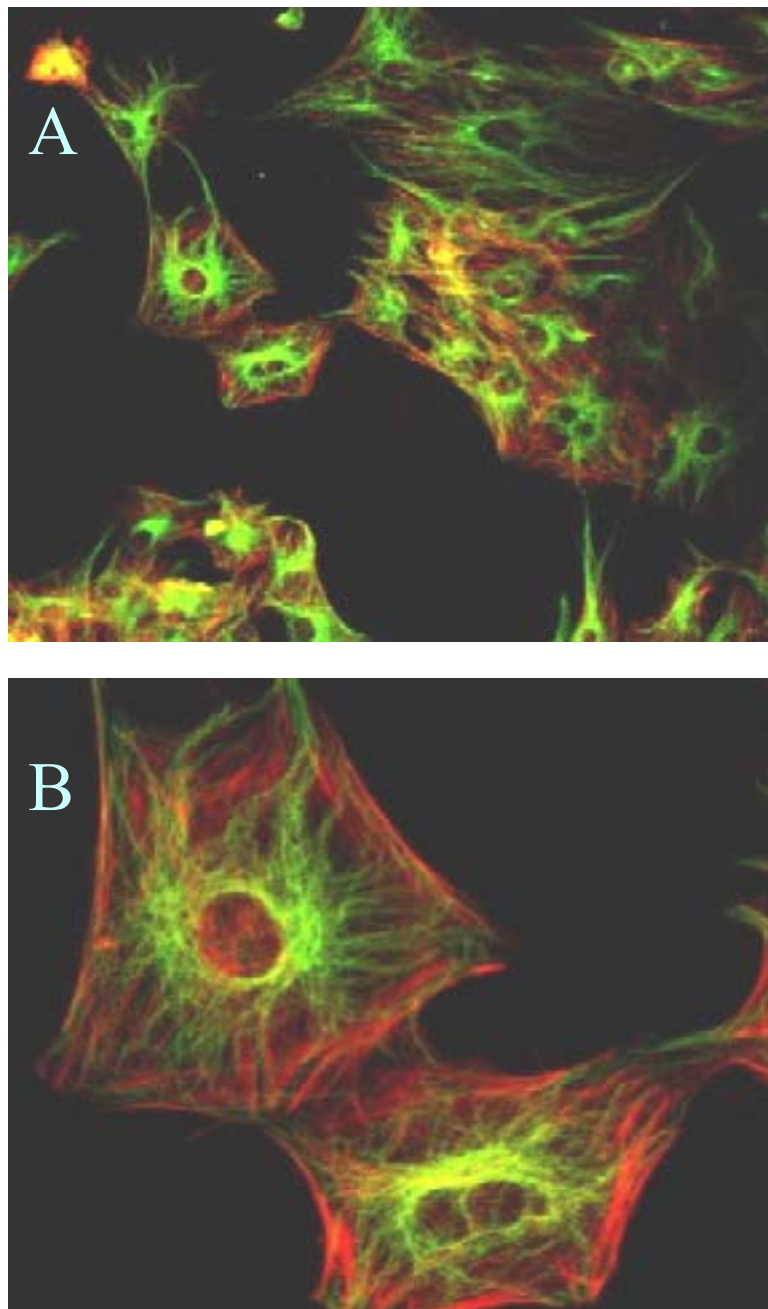


Figure 3.1 Immunofluorescence visualization of actin filaments (red in color) and tubulin filaments (green in color) (A) 400 magnification (B) 630 magnification.

Cytotoxicity Evaluation of Cytochalasin D

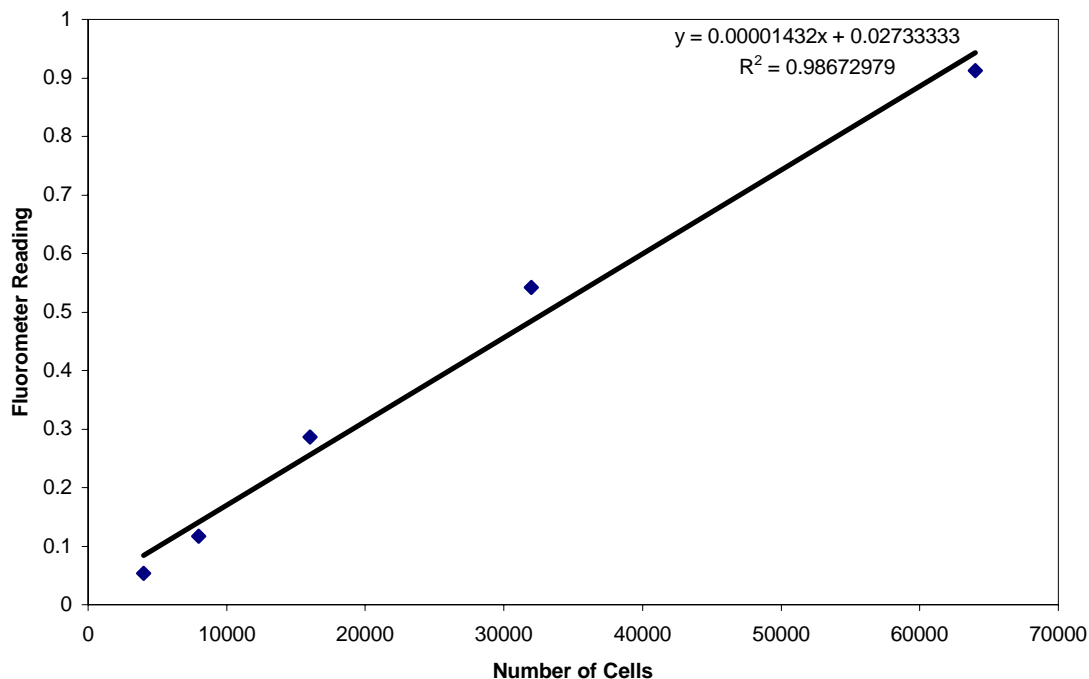


Figure 3.2 Standard Curve using CellTiter 96® AQueous One Solution Cell Proliferation Assay.

Cytochalasin D Conc. (μ M)	Fluorometric Reading	Number of Cells
1	1.319	54120
2	1.191	48757
3	0.701	47043
4	0.711	47742
5	0.811	54725
10	1.051	71485
15	1.097	74697
20	0.620	41387

Table 3.1 Toxicity effects of varying concentration of Cytochalasin D on C3H10T1/2 cells

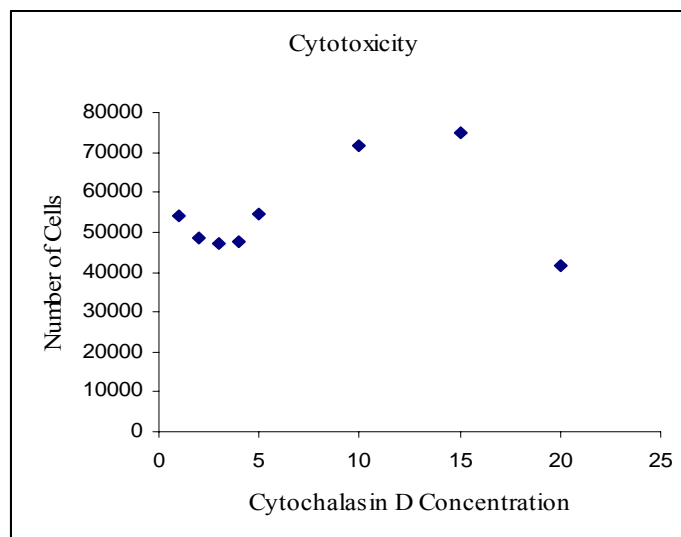


Figure 3.3 Cytochalasin D cytotoxicity readings scatter plot.

Toxicity effects of varying concentrations of Cytochalasin D on C3H10T1/2 cells were counted as cell viability and were observed after 3 days using the CellTiter 96® AQueous One Solution Cell Proliferation Assay. The cells were cultured at a seeding density of 25,000 cells and exposed to a specific concentration of Cytochalasin D for 2 hours per day.

Linear model: Number of Cells = 52250.6 + 365.852*Cytochalasin					
Parameter	Estimate	Standard Error	t-Statistic	P-Value	
Intercept	52250.6	6863.65	7.61266	0.0003	
Slope	365.852	695.109	0.526323	0.6175	
Correlation	R-Squared	Adjusted R-Squared	Residual Std. Error	MAE	Durbin-Watson
0.210076	4.41318	-11.518	12627.3	8670.79	1.6104

Table 3.2 Linear correlation model for evaluating cytotoxicity of Cytochalasin D on C3H10T1/2 cells.

A linear correlation model was used to describe the relationship between cell number and Cytochalasin D concentration. The equation of the fitted model was as follows: $\text{Number of Cells} = 52250.6 + 365.852 \times [\text{Cytochalasin D}]$

Results from this model are shown in Table 3.2 and indicate that since the P-value for the slope is greater or equal to 0.05, there is not a statistically significant relationship between the number of cells present and Cytochalasin D concentration at the 95.0% confidence level. Additionally, the R-Squared statistic indicates that the model as fitted explains 4.41% of the variability in the number of cells. The correlation coefficient equals 0.2101, indicating a relatively weak relationship between the variables.

Cytochalasin D Induced Disruption of Actin Filaments

Cytochalasin D depolymerizes actin filaments, and its effect was characterized for time and duration of treatment on C3H10T1/2 cells. In cytotoxicity studies the drug was found to be non-toxic to C3H10T1/2 cells for up to 3 days for concentrations ranging from 0.1 μM to 20 μM . The minimum concentration and time required for disruption of actin filaments was determined in this experiment. Zanetti and Solursh (1984) treated the chick limb bud cells with Cytochalasin D for 3 to 24 hours with successful disruption of actin filaments. After this treatment cells were examined by scanning electron microscopy. Representative areas of the cultures were photographed, and all cells scored as flattened, round, or bipolar. At least 300 cells were counted for each treatment.

Concentration of Cytochalasin D (μM)	Rounded Cells (%)
0	32.6
0.02	43.7
0.2	51.2
2.0	78.7
4.0	96.5

Table 3.3 Effects of various concentrations of Cytochalasin D on cell shape (actin disruption) in Chick Limb Bud Cells. (Zanetti and Solursh, 1984)

For C3H10T1/2 cells, we chose to treat the cells for 2 hours to determine the effect. Zanetti and Solursh (1984) also found that the lower concentrations (0.02 μM to 2.0 μM) of Cytochalasin D are insufficient to disrupt all the actin filaments. Therefore, we chose to treat the C3H10T1/2 cells with Cytochalasin D at concentrations of 2 μM , 4 μM and 8 μM , to compare with the untreated cells. The actin disruption effects were studied using actin specific phalloidin phalloxin and visualized using immunofluorochemistry as shown in figure 3.4.

Normal actin filaments are smooth and continuous (Fig. 3.4 A). With the addition of 2 μM Cytochalasin D, some of the actin fibers were disrupted, but some intact filaments can still be observed. Treatment with 4 μM Cytochalasin D disrupted the filaments almost completely. Many bright green spots are visible. This can be attributed to the depolymerization and consolidation of actin monomers. Extrapolating from the results obtained by Zanetti and Solursh (1984), it was determined that the actin disruption by 2 μM Cytochalasin D is almost 80% and almost 98% by 4 μM Cytochalasin D. Treatment with 8 μM Cytochalasin D did not increase actin disruption significantly over

that of the 4 μM Cytochalasin D treatment; however, it was concluded that the actin monomers were more uniformly distributed. Therefore, for subsequent experiments, a minimum of 2 hours treatment time with 4 μM Cytochalasin D was chosen.

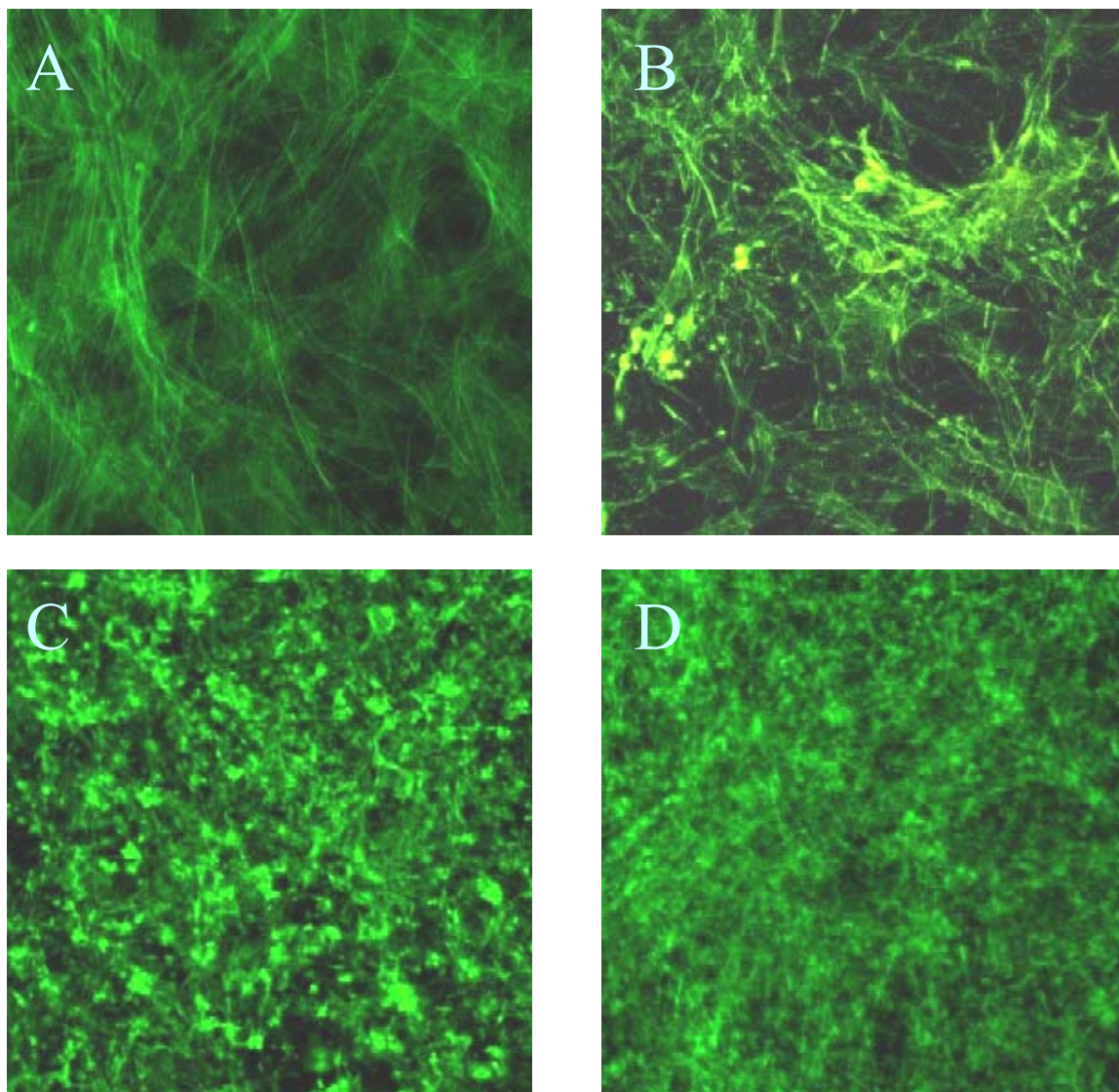


Figure 3.4 Effect of various concentrations of Cytochalasin D on actin disruption in C3H10T1/2 cells treated for 2 hr. (400 magnification). Smooth and continuous actin fibers (A; Control) are compared with Cytochalasin D induced actin disruption with progressive concentrations (B, C and D; 2, 4, 8 μM Cytochalasin D respectively)

Reversible Effect of Cytochalasin D

In this experiment the ability of cells to re-polymerize actin monomers to regain and reorganize actin filaments after removal of Cytochalasin D was examined. The reversible or irreversible effect of Cytochalasin D is the determining factor for the design of the hydrostatic pressurization experiment. To examine the effect, C3H10T1/2 cells were treated with Cytochalasin D for 24 hrs. The drug was washed off, and the cells were cultured in a drug free medium for 24 hrs after which they were fixed and studied by immunofluorescence microscopy. Results are shown in figure 3.5.

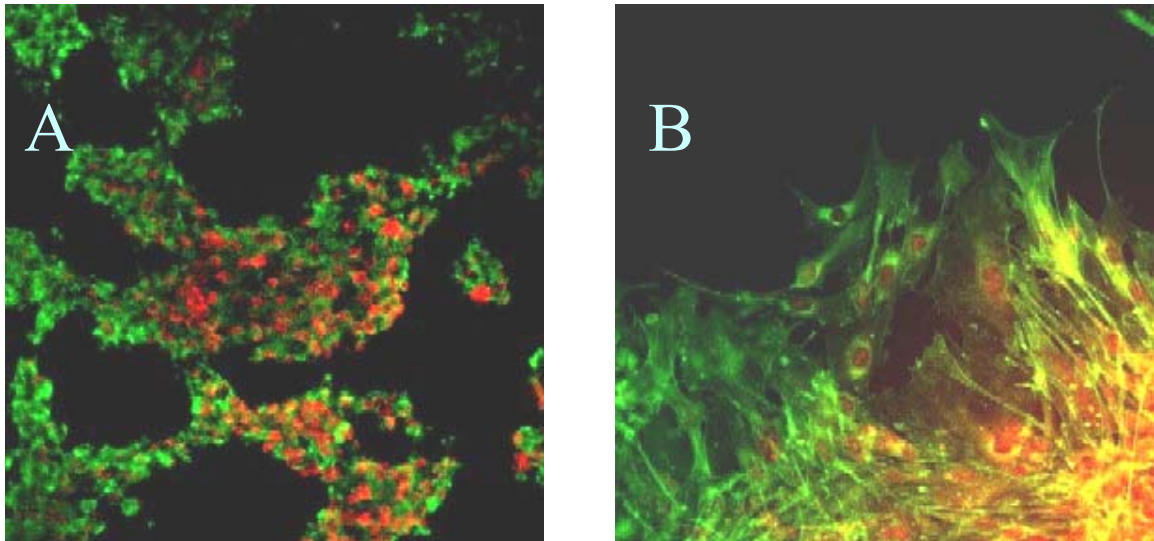


Figure 3.5 Reversible effect of Cytochalasin D on actin disruption. (A) Effect of Cytochalasin D on actin disruption in C3H10T1/2 cells treated for 24 hr. (B) Actin reorganization in Cytochalasin D treated C3H10T1/2 cells 24 hr after removal of drug.

C3H10T1/2 cells were found to regain and reorganize the actin filaments completely within 24 hr after removal of Cytochalasin D. In hydrostatic pressurization experiments, the drug treated pressurized cells were maintained in a drug free culture

medium for 5 days with daily supplements of ascorbic acid so as to facilitate the cells to produce cartilaginous extracellular matrix proteins. Since extracellular matrix proteins are correlated to actin filaments in intracellular signaling, the presence of the cellular actin filaments in the latter 5 days of pressure relaxation is essential to avoid doubt in the cellular mechanism. The reversible effect of Cytochalasin D assures the reorganization of actin filaments that are essential to extracellular matrix related intracellular signaling.

Chondrogenic Effects of Actin Disruption

Because the overall study aims to investigate the role of actin filaments in chondroinduction by hydrostatic pressurization using Cytochalasin D induced actin disruption as a tool, it was important to investigate whether disruption of actin filaments alone can induce chondrogenesis. For hydrostatic pressurization, the cells were allowed to adhere for first 24 hours before pressurization with or without Cytochalasin D. Therefore, to investigate the chondrogenic effects of actin disruption, the cells were treated with Cytochalasin D for second 24 hr.

Immunofluorescence

The cells were assigned to one of the 4 groups: control (no BMP-2 or Cytochalasin D), 100 ng/ml BMP-2, 4 μ M Cytochalasin D, or a combined treatment of 100 ng/ml BMP-2 and 4 μ M Cytochalasin D. High-density micromass spot cultures made it difficult to view individual cells in immunofluorescence studies. Therefore, the center

of the micromass culture at 100 magnification and the edge at 400 magnification are shown here (Fig. 3.6, Fig. 3.7 and Fig. 3.8).

The BMP-2 treated culture did not show any difference against the control culture in the immunofluorescence study (Fig. 3.6 and Fig. 3.7). However, other qualitative and quantitative techniques proved the differences as shown later. In those cells exposed to Cytochalasin D throughout the entire culture period, the cells remained rounded and proliferated far less than controls (Fig. 3.8 A). In the culture from which the Cytochalasin D was removed after 24 hours, the actin cytoskeleton structure was regenerated and reorganized within 24 hours (Fig. 3.8 B). In the combination group (BMP-2 and Cytochalasin D), the immunofluorescence finding was similar to the group with Cytochalasin D only.

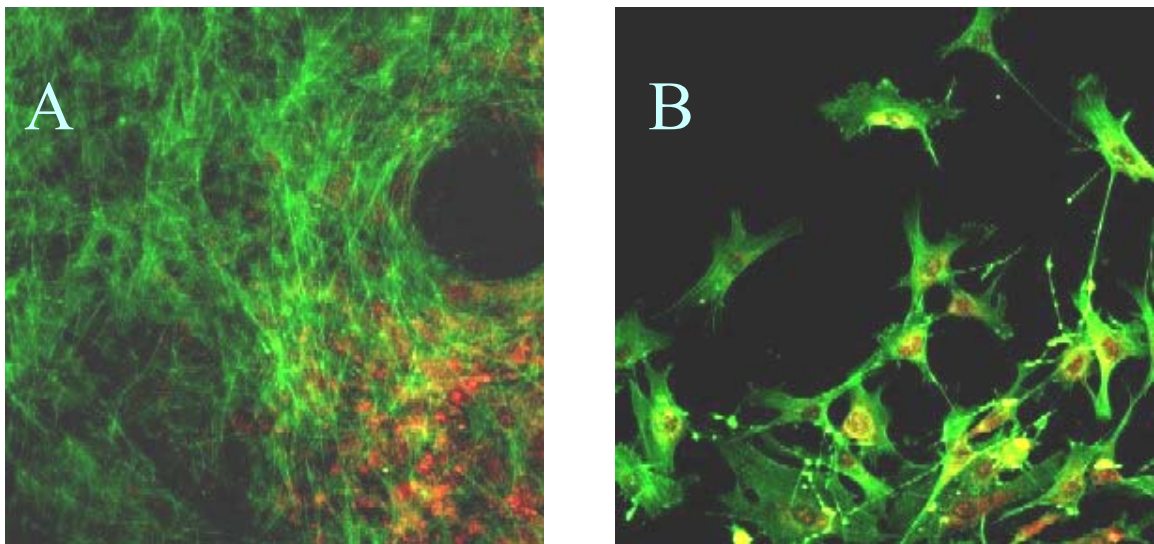


Figure 3.6 Phalloidin-Propidium Iodide staining of C3H10T1/2 cells after 48 hours micromass culture. (A) Control (no BMP-2 or Cytochalasin D) 100 magnification at the center of micromass. (B) Control (no BMP-2 or Cytochalasin D) 400 magnification at the edge of micromass.

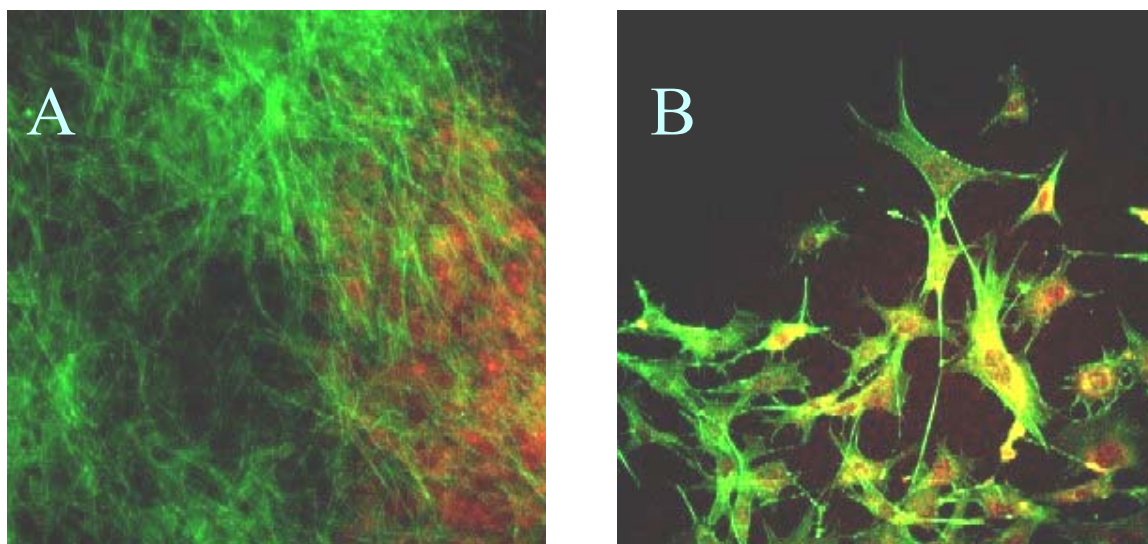


Figure 3.7 Phalloidin-Propidium Iodide staining of C3H10T1/2 cells after 48 hours micromass culture. (A) BMP-2, 100 magnification at center. (B) BMP-2, 400 magnification at the edge.

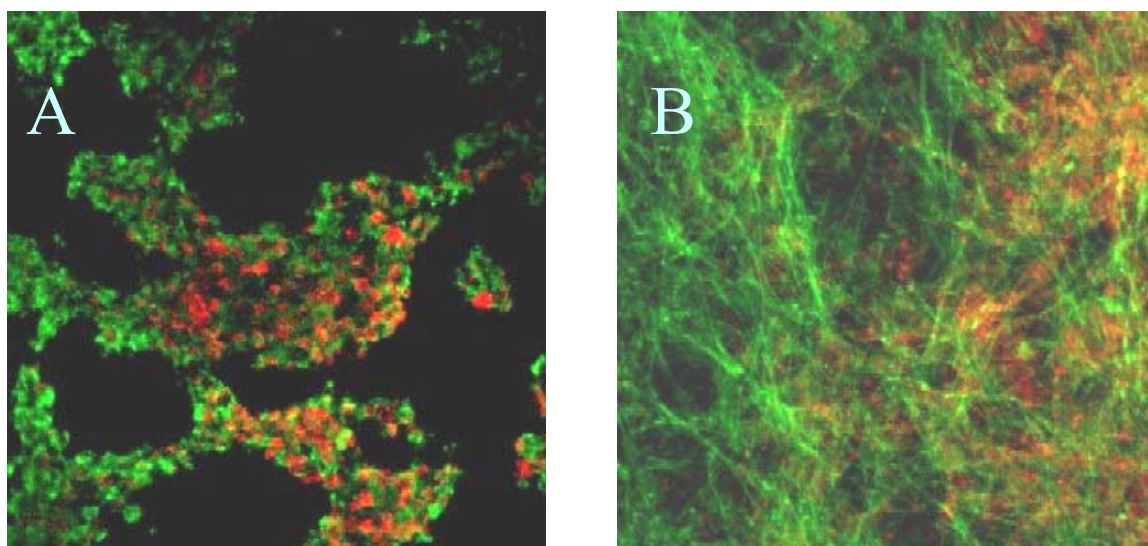


Figure 3.8 Phalloidin and Propidium Iodide staining of Cytochalasin D treated C3H10T1/2 cells after 48 hours in micromass culture. (A) Continuous exposure to 4 μ M Cytochalasin D, (100 magnification). (B) Initial 24-hour exposure to 4 μ M Cytochalasin D, (100 magnification)

Toluidine Blue Staining of Glycosaminoglycan (Qualitative Analysis)

Toluidine-blue specifically stains glycosaminoglycans showing a violet color. Cells treated with 100 ng/ml BMP-2 for 12 days displayed metachromatic staining toluidine blue (Fig. 3.9), indicating a high glycosaminoglycan concentration. Such metachromasia was not observed in control cells or in either group treated continuously with Cytochalasin D (Fig. 3.9).

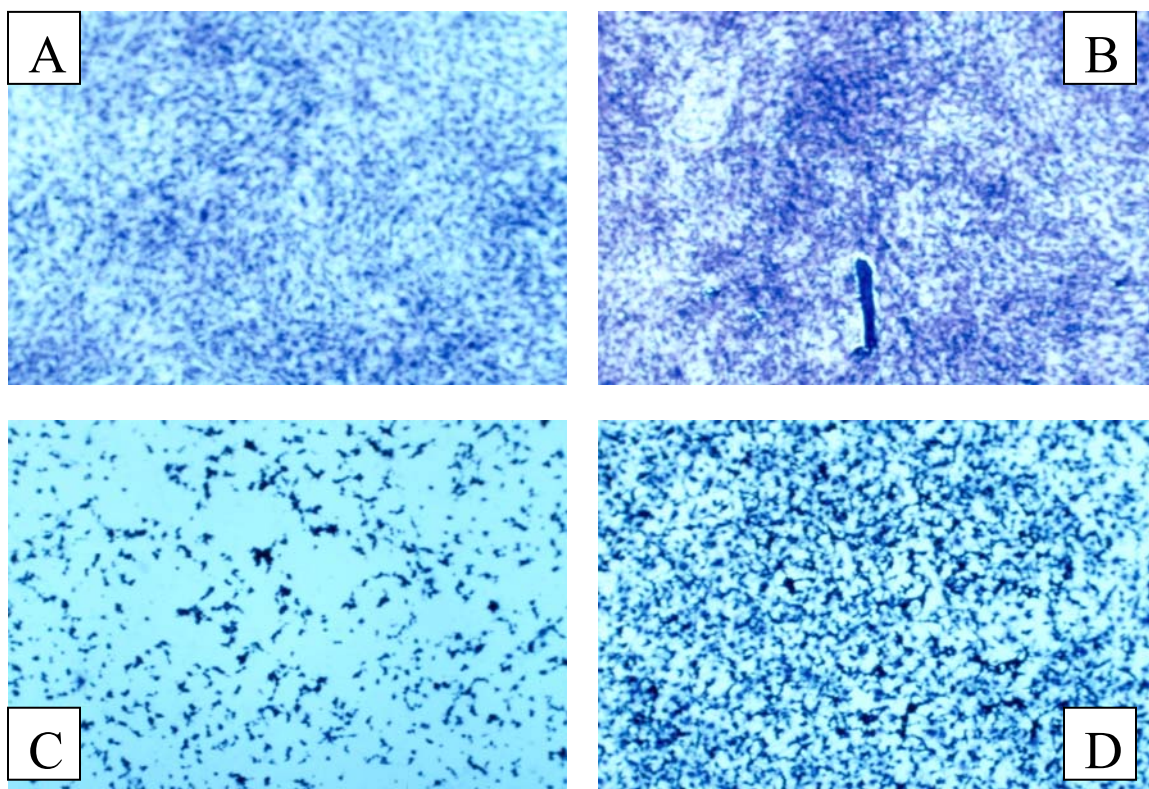


Figure 3.9 Day 12 toluidin-blue stained cultures (40 magnification). (A) Control, (B) BMP-2, (C) Continuous exposure to Cytochalasin D, (D) Continuous exposure to BMP-2 and Cytochalasin D.

Statistical Analysis of Sulfated Glycosaminoglycan (Quantitative Analysis)

Sulfated glycosaminoglycan (sGAG) and DNA were quantified for 8 samples of each of the 4 groups. The sGAG reading ($\mu\text{g}/\text{sample}$) was normalized to the respective DNA reading ($\mu\text{g}/\text{sample}$) and sGAG/DNA ($\mu\text{g}/\mu\text{g}$) readings for each sample were used for two-way ANOVA statistical analysis. StatletsTM software was used for statistical analysis. Two-way ANOVA analysis was performed on the 4 groups using BMP-2 (100 ng/ml) and Cytochalasin D (4 μM) as concentration variables [i.e. Control (0:0), BMP-2 (100:0), Cytochalasin D (0:4) and BMP-2 & Cytochalasin D (100:4)].

ANOVA Table - Type III Sums of Squares					
Response variable: sGAG/DNA					
Source	Sum of Squares	D.F.	Mean Square	F-Ratio	P-Value
BMP-2	6.83936	1	6.83936	10.77	0.0028
Cytochalasin	0.285296	1	0.285296	0.45	0.5081
INTERACTION	0.00160037	1	0.00160037	0.00	0.9603
RESIDUAL	17.7749	28	0.634816		
Total (corr.)	24.9011	31			

Table 3.4 Two-way ANOVA table for sGAG/DNA readings analyzing chondroinductive effect of BMP-2 and Cytochalasin D.

The ANOVA table (Table 3.4) decomposes the variance of the data into four components: a component due to differences between levels of BMP-2, a component due to differences between levels of Cytochalasin D, a component due to interactions between BMP-2 and Cytochalasin D, and a residual component. F-tests were run to determine which factors were statistically significant. The BMP-2 group have P-value below 0.05 and indicate statistically significant effects on sGAG/DNA synthesis.

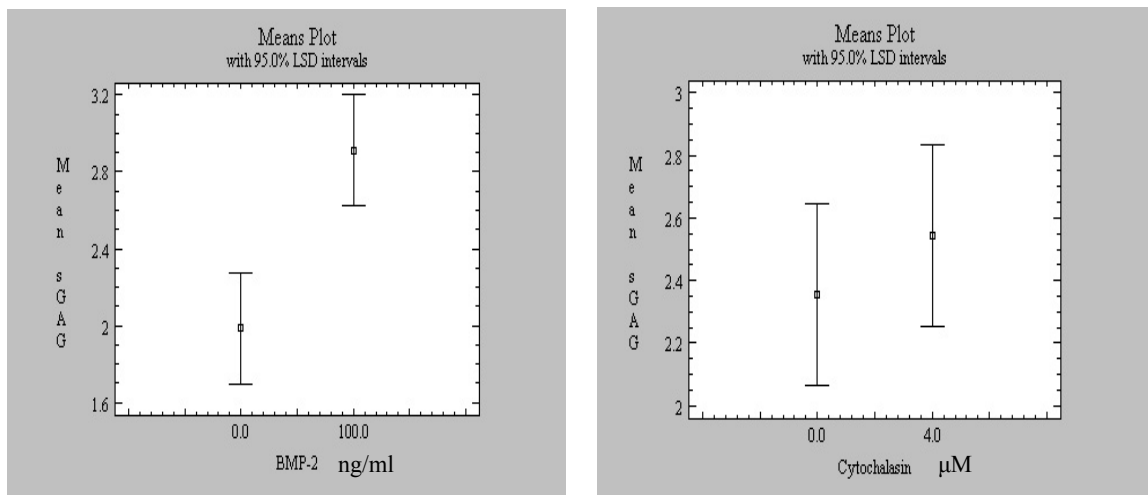


Figure 3.10 Means plot for sGAG/DNA readings analyzing chondroinductive effect of BMP-2 and Cytochalasin D.

The means plots (Fig. 3.10) show the mean for each level of BMP-2 and Cytochalasin D. It also displays an interval around each mean. The intervals currently displayed are based on Fisher's least significant difference (LSD) procedure. They are constructed in such a way that if two means are the same, their intervals will overlap 95.0% of the time.

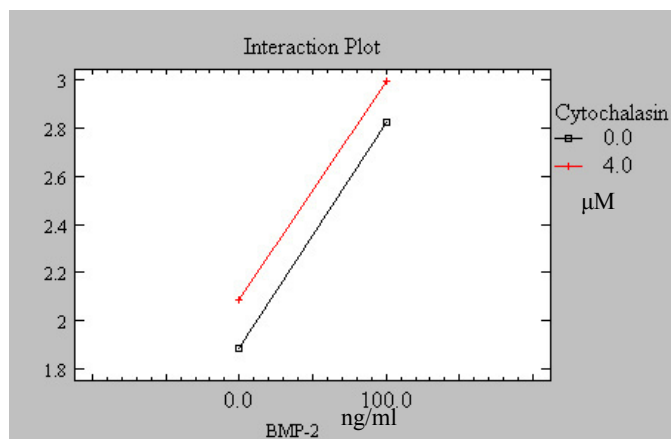


Figure 3.11 Interaction plot for BMP-2 and Cytochalasin D with respect to chondroinductive effect measured as sGAG/DNA.

Fig 3.11 shows an interaction plot that is useful for interpreting the interaction between BMP-2 and Cytochalasin D. The two lines drawn on the graph represent each of the levels of Cytochalasin D. They connect the least squares means for the two levels of BMP-2. If there was absolutely no interaction, these lines would be parallel. The stronger the interaction, the more different the shape of the lines.

Chondrogenic Effects of Short Duration Hydrostatic Pressurization

A hydrostatic pressurization system for inducing chondrogenesis in C3H10T1/2 cells was essential for hypothesis testing. Therefore, short and long duration hydrostatic pressure applied at a physiological range of 5 MPa was tested for chondrogenic system. In the short duration testing, the cells, cultured in 3 X 4 sections of a round bottom 96-well plate, were pressurized for 1 hour per day with 10 minutes pressurization and 10 minutes rest cycle for 3 consecutive days. The cells were maintained in an incubator for an additional 5 days with daily addition of ascorbic acid.

Statistical Analysis for sGAG/DNA

Sulfated glycosaminoglycan (sGAG) and DNA were quantified for 10 samples of control (non-pressurized) and experimental groups (pressurized). The sGAG reading ($\mu\text{g}/\text{well}$) was normalized to the respective DNA reading ($\mu\text{g}/\text{well}$) and sGAG/DNA ($\mu\text{g}/\mu\text{g}$) readings for each sample were statistically analyzed using a student's t-test for two independent samples. StatletsTM software was used for statistical analysis.

Comparison of Population Means					
	Sample Size	Sample Mean	Lower 95.0% Conf. Limit	Upper 95.0% Conf. Limit	Sample Std. Deviation
Control	10	0.65548	0.465852	0.845108	0.265081
Experimental	10	0.62544	0.472097	0.778783	0.214358
Difference		0.03004	-0.196449	0.256529	
t-Test					
Null Hyp.	Alt. Hyp.	Test Statistic	P-Value		
0.0	Not equal	0.28	0.7837		
Do not reject the null hypothesis at the 5.0% significance level.					

Table 3.5 Student's t-test for sGAG/DNA readings, comparing population means for control (non-pressurized) and experimental (pressurized) independent samples, analyzing chondroinductive effect of short duration hydrostatic pressurization.

Comparison of Population Standard Deviations				
	Sample Size	Sample Sigma	Lower 95.0% Conf. Limit	Upper 95.0% Conf. Limit
Control	10	0.265081	0.182332	0.483935
Experimental	10	0.214358	0.147443	0.391334
Ratio		1.23663	0.379844	6.15675
F Test				
Null Hyp.	Alt. Hyp.	Test Statistic	P-Value	
1.0	Not equal	1.53	0.5369	
Do not reject the null hypothesis at the 5.0% significance level.				

Table 3.6 F-test for radioactive counts per minute readings, comparing population standard deviations for control (non-pressurized) and experimental (pressurized) independent samples, analyzing chondroinductive effect of short duration hydrostatic pressurization.

Table 3.5 displays the result of a t-test performed to test the null hypothesis that the difference of sGAG/DNA synthesis between the means of the populations from which the two samples come equals 0.0 versus the alternative hypothesis that the difference is not equal to 0.0. Since the P-value for this test is greater than or equal to 0.05, we cannot

reject the null hypothesis at the 95.0% confidence level. Therefore, the sGAG/DNA means for control and experimental groups does not differ significantly. Also shown is a 95.0% confidence interval for the difference between the population means. In repeated sampling, 95.0% of all such intervals will contain the true difference.

Table 3.6 displays the result of the F test performed to test the null hypothesis that the ratio of the variances of the populations from which the two samples come equals 1.0 versus the alternative hypothesis that the ratio is not equal to 1.0. Since the P-value for this test is greater than or equal to 0.05, we cannot reject the null hypothesis at the 95.0% confidence level. Therefore, the sGAG/DNA variances for control and experimental groups do not differ significantly. Also shown is a 95.0% confidence interval for the ratio of the population variances. In repeated sampling, 95.0% of all such intervals will contain the true ratio. The F-test and confidence interval shown here depend on the samples having come from normal distributions.

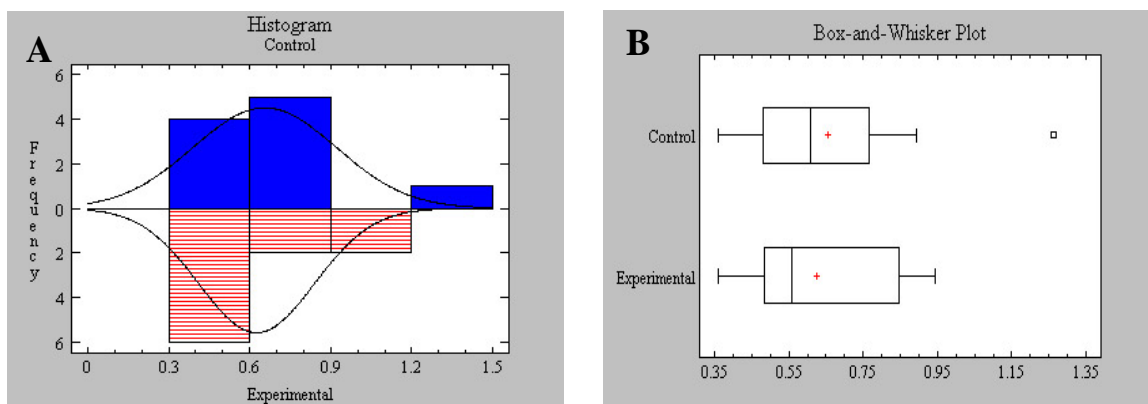


Figure 3.12 The sample distribution plots for sGAG/DNA readings comparing control (non-pressurized) and experimental (pressurized) groups subjected to short duration hydrostatic pressure. (A) Histogram (B) Box-and-whisker plot.

The graphs (Fig. 3.12 A and B) show histogram and box-and-whisker plots for both control and experimental groups. The histogram shows a normal distribution of the sGAG/DNA readings for both groups. The skewness and the kurtosis are observed to be low for both groups affirming near normal distribution that can be used for the F test. The box-and-whisker plots show various features of both the groups. The rectangular part of the plot extends from the lower quartile to the upper quartile, covering the center half of the sample. The center line within the box shows the location of the sample median. The plus sign indicates the location of the sample mean. The whiskers extend from the box to the minimum and maximum values in the sample, except for any outside or far outside points, which are plotted separately as small squares.

Statistical Analysis: Rate of Collagen Synthesis

The rate of collagen synthesis was quantified for 9 samples of control (non-pressurized) and experimental groups (pressurized) by a ³H Proline radioactive assay. The scintillation readings (measured as counts per minute) for each sample were statistically analyzed using student's t-test for the two independent samples.

Table 3.7 displays the result of a t-test performed to test the null hypothesis that the difference of rate of collagen synthesis between the means of the populations from which the two samples come equals 0.0 versus the alternative hypothesis that the difference is not equal to 0.0. Since the P-value for this test is greater than or equal to 0.05, we cannot reject the null hypothesis at the 95.0% confidence level, showing that there was no significant difference between sGAG/DNA synthesis of control and experimental groups.

Comparison of Population Means					
	Sample Size	Sample Mean	Lower 95.0% Conf. Limit	Upper 95.0% Conf. Limit	Sample Std. Deviation
Control	9	4589.17	3632.24	5546.11	1244.93
Experimental	9	5346.85	4758.18	5935.52	765.826
Difference		-757.677	-1790.51	275.158	
t-Test					
Null Hyp.	Alt. Hyp.	Test Statistic	P-Value		
0.0	Not equal	-1.56	0.1395		
Do not reject the null hypothesis at the 5.0% significance level.					

Table 3.7 Student's t-test for radioactive counts per minute readings, comparing means for control (non-pressurized) and experimental (pressurized) independent samples, analyzing rate of collagen synthesis of C3H10T1/2 cells subjected to short duration hydrostatic pressurization.

Comparison of Population Standard Deviations				
	Sample Size	Sample Sigma	Lower 95.0% Conf. Limit	Upper 95.0% Conf. Limit
Control	9	1244.93	840.895	2384.99
Experimental	9	765.826	517.282	1467.14
Ratio		1.6256	0.596081	11.7152
F Test				
Null Hyp.	Alt. Hyp.	Test Statistic	P-Value	
1.0	Not equal	2.64	0.1909	
Do not reject the null hypothesis at the 5.0% significance level.				

Table 3.8 F-test for radioactive counts per minute readings, comparing population standard deviations for control (non-pressurized) and experimental (pressurized) independent samples, analyzing rate of collagen synthesis of C3H10T1/2 cells subjected to short duration hydrostatic pressurization.

Table 3.8 displays the result of the F test performed to test the null hypothesis that the ratio of the variances of the populations from which the two samples come equals 1.0 versus the alternative hypothesis that the ratio is not equal to 1.0. The samples were

found to be near normal distributed. Since the P-value for this test is greater than or equal to 0.05, we cannot reject the null hypothesis at the 95.0% confidence level or, in other words, the two groups have equal variances.

Collagen Type II Immunostaining

Two wells per control (non-pressurized) and experimental (pressurized) groups were stained with II-II6B3 antibody for type II collagen. One well per group was not stained with the antibody and was treated as the control for immunostaining. Figure 3.13 shows the results from this assay.

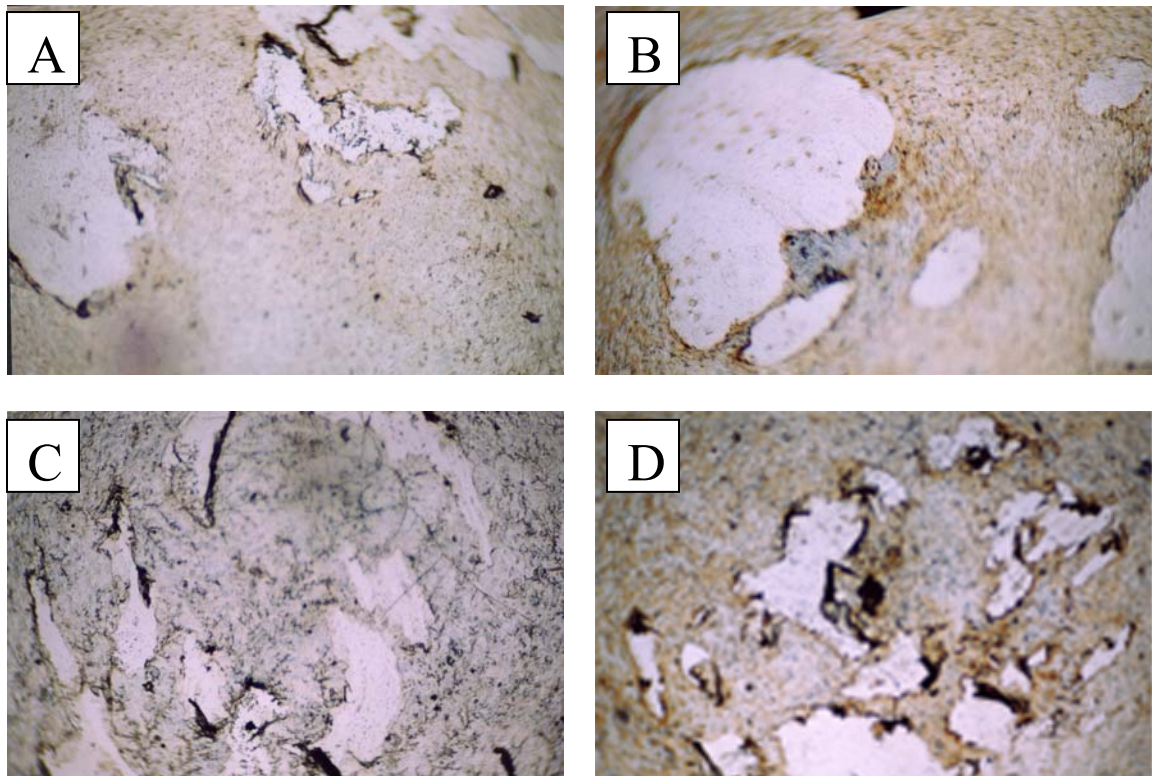


Figure 3.13 Collagen type II immunostaining in micromass cultures of C3H/10T1/2 cells. A-B: Control, C-D: pressurized. Primary antibody was omitted from A and C.

Alcian Blue Staining

Two wells per control (non-pressurized) and experimental (pressurized) groups were stained with alcian blue for glycosaminoglycan staining. It was difficult to get a good full view image with proper focus due to curved surface. Therefore, the images were taken by inverting the wells and photographing the bottoms of the wells. Visually the Alcian Blue staining between control and experimental groups appeared similarly (Fig. 3.14).

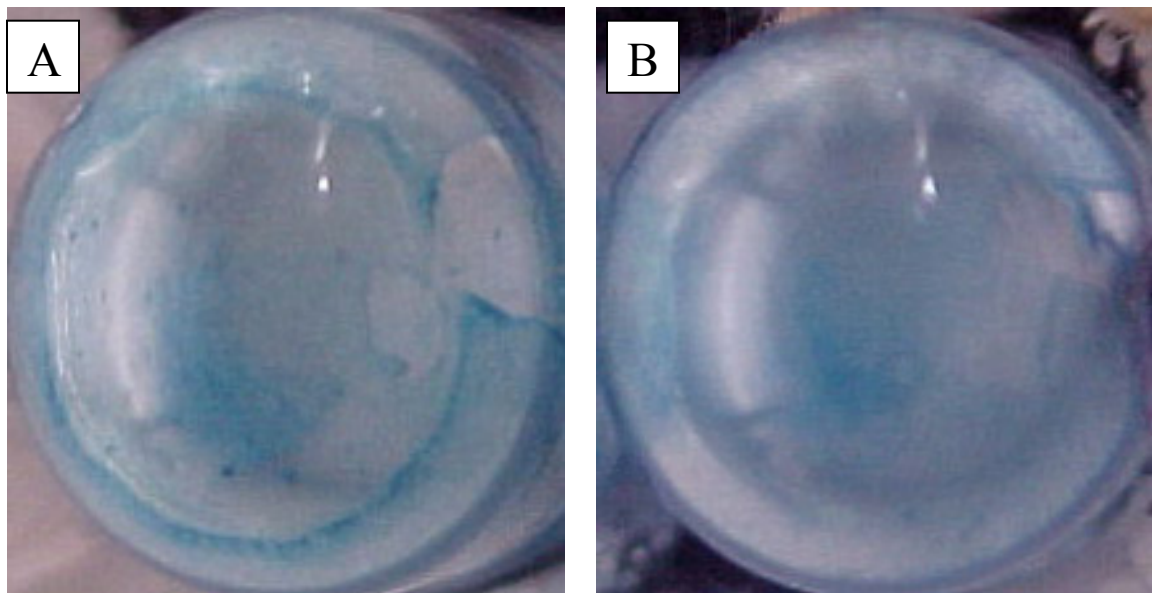


Figure 3.14 Alcian blue histochemical staining for glycosaminoglycan in samples for testing chondroinductive effect of short duration hydrostatic pressurization. (A) Control (non-pressurized) (B) Experimental (Pressurized).

Chondrogenic Effects of Long Duration Hydrostatic Pressurization

In the long duration testing, the cells, cultured in 3 X 4 sections of a round bottom 96-well plate, were pressurized for 4 hours per day with 10 minutes pressurization and 10 minutes rest cycle for 3 consecutive days. The cells were maintained in an incubator for an additional 5 days with daily additions of ascorbic acid.

Statistical Analysis for sGAG/DNA

sGAG and DNA were quantified and normalized for 10 samples from the control and experimental groups as previously described. The sGAG/DNA ($\mu\text{g}/\mu\text{g}$) readings for were statistically analyzed using a student's t-test for two independent samples.

Comparison of Population Means					
	Sample Size	Sample Mean	Lower 95.0% Conf. Limit	Upper 95.0% Conf. Limit	Sample Std. Deviation
Control	8	1.14785	0.851216	1.44448	0.354816
Experimental	9	2.21528	2.01113	2.41943	0.265591
Difference		-1.06743	-1.38895	-0.745908	
t-Test					
Null Hyp.	Alt. Hyp.	Test Statistic	P-Value		
0.0	Not equal	-7.08	0.0000		
Reject the null hypothesis at the 5.0% significance level.					

Table 3.9 Student's t-test for sGAG/DNA readings, comparing means for control (non-pressurized) and experimental (pressurized) independent samples, analyzing chondroinductive effects of long duration hydrostatic pressurization.

Table 3.9 displays the result of a t-test performed to test the null hypothesis that the difference of sGAG synthesis between the means of the populations from which the

two samples come equals 0.0 versus the alternative hypothesis that the difference is not equal to 0.0. Since the P-value for this test is less than 0.05, we can reject the null hypothesis at the 95.0% confidence level and accept the alternate hypothesis. In the t-test analysis, two readings were excluded from control group and one reading was excluded from experimental group because these readings represented statistical outliers as shown by box plots (Fig. 3.15 A and C). The outliers were assumed to be experimental or sampling errors. Inclusion or exclusion of outliers did not change the final conclusion of the t-test and other statistical tests.

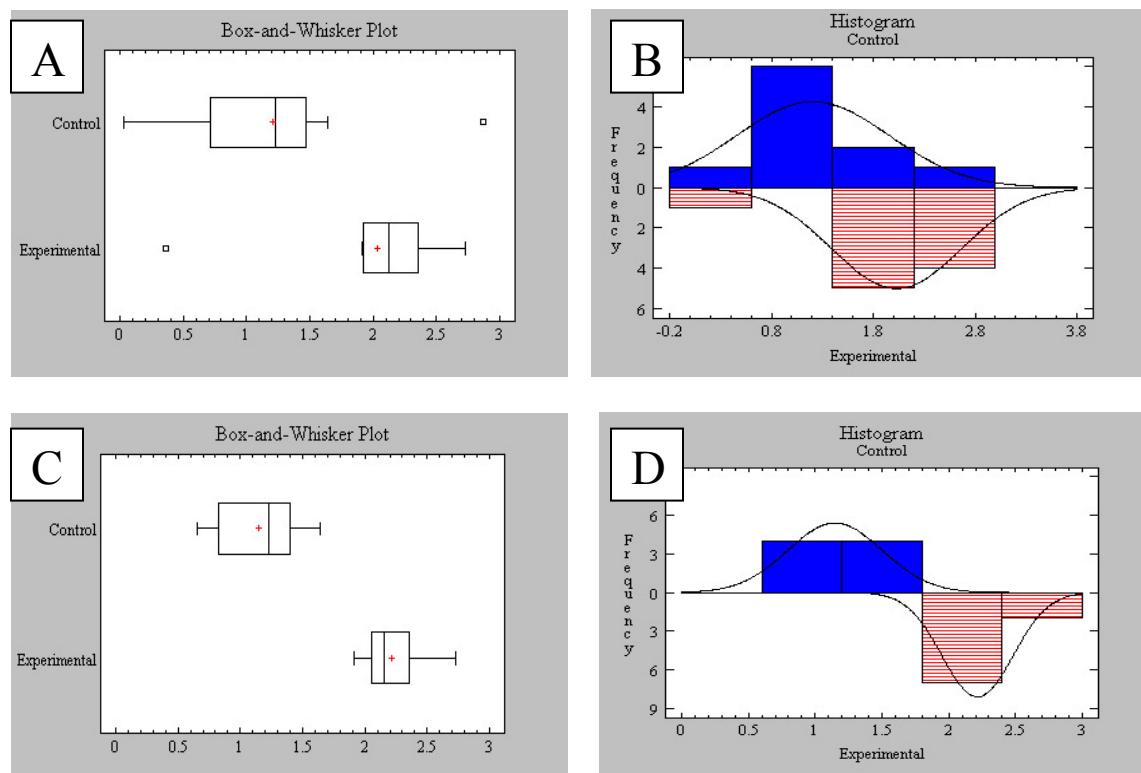


Figure 3.15 The sample distribution plots for sGAG/DNA readings comparing control (non-pressurized) and experimental (pressurized) groups subjected to long duration hydrostatic pressure. (A and C) Box-and-whisker plot, (B and D) Histogram. (A and B) with outliers, (C and D) without outliers.

Table 3.10 displays the result of the F-test and proves the null hypothesis that the ratio of the variances of the populations from which the two samples come equals 1.0. The samples were near normal distribution as shown in Fig 3.15 D. Since the P-value for this test is greater than or equal to 0.05, we cannot reject the null hypothesis at the 95.0% confidence level. Therefore, both control and experimental groups have equal variances.

Comparison of Population Standard Deviations				
	Sample Size	Sample Sigma	Lower 95.0% Conf. Limit	Upper 95.0% Conf. Limit
Control	8	0.354816	0.234595	0.722147
Experimental	9	0.265591	0.179395	0.50881
Ratio		1.33595	0.394113	8.74416
F Test				
Null Hyp.	Alt. Hyp.	Test Statistic	P-Value	
1.0	Not equal	1.78	0.4343	
Do not reject the null hypothesis at the 5.0% significance level.				

Table 3.10 F-test for sGAG/DNA readings, comparing population standard deviations for control (non-pressurized) and experimental (pressurized) independent samples, analyzing chondroinductive effect of long duration hydrostatic pressurization.

Statistical Analysis: Rate of Collagen Synthesis

The rate of collagen synthesis was quantified for 9 samples of the control (non-pressurized) and experimental groups (pressurized) by a 3H Proline radioactive assay. The scintillation readings measured as counts per minute for each sample were statistically analyzed using a student's t-test for the two independent samples (Table 3.11). One outlier was excluded from each group as experimental or sampling error. The two groups did not have equal variances as shown by the F-test performed (Table 3.12).

Therefore the t-test was performed using pooled variances. Since the P-value for t-test is less than 0.05, the two groups have significantly different population means. It can be observed that the experimental (pressurized) group has significantly greater sGAG/DNA synthesis than the control (non-pressurized) group.

Comparison of Population Means					
	Sample Size	Sample Mean	Lower 95.0% Conf. Limit	Upper 95.0% Conf. Limit	Sample Std. Deviation
Control	8	4905.33	3776.76	6033.9	1349.93
Experimental	8	11029.9	6440.58	15619.2	5489.48
Difference		-6124.58	-10749.5	-1499.63	
t-Test					
Null Hyp.	Alt. Hyp.	Test Statistic	P-Value		
0.0	Not equal	-3.06	0.0159		
Reject the null hypothesis at the 5.0% significance level.					

Table 3.11 Student's t-test for radioactive counts per minute readings, comparing means for control (non-pressurized) and experimental (pressurized) independent samples, analyzing rate of collagen synthesis in long duration hydrostatic pressurization.

Comparison of Population Standard Deviations				
	Sample Size	Sample Sigma	Lower 95.0% Conf. Limit	Upper 95.0% Conf. Limit
Control	8	1349.93	892.538	2747.47
Experimental	8	5489.48	3629.5	11172.6
Ratio		0.245912	0.0121069	0.302055
F Test				
Null Hyp.	Alt. Hyp.	Test Statistic	P-Value	
1.0	Not equal	0.06	0.0015	
Reject the null hypothesis at the 5.0% significance level.				

Table 3.12 F-test for radioactive counts per minute readings, comparing population standard deviations for control (non-pressurized) and experimental (pressurized) independent samples, analyzing rate of collagen synthesis of C3H10T1/2 cells subjected to long duration hydrostatic pressurization.

Collagen Type II Immunostaining

Two wells per control (non-pressurized) and experimental (pressurized) groups were stained with II-II6B3 antibody for type II collagen. One well per group was not stained with the antibody and was treated as the control for immunostaining. Fig 3.16 shows the results from this assay.

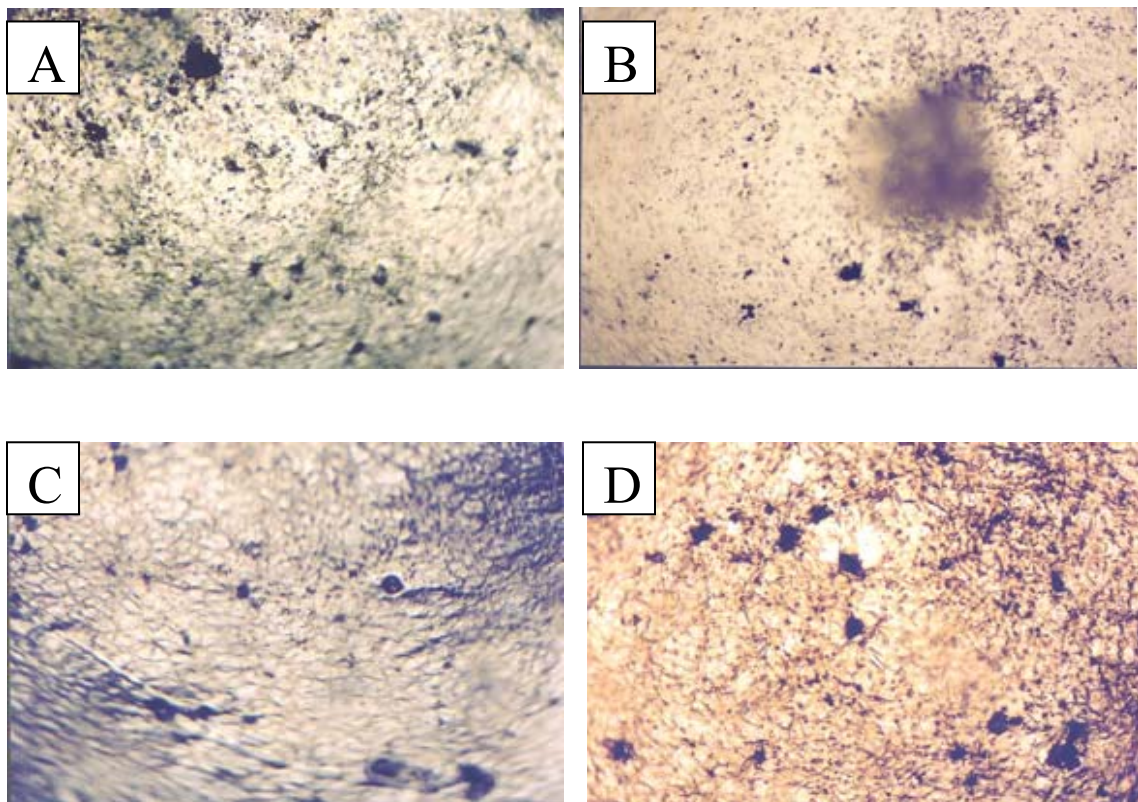


Figure 3.16 Collagen type II immunostaining in micromass cultures of C3H/10T1/2 cells hydrostatically pressurized for long duration (4X). A-B: Control, C-D: pressurized. Primary antibody was omitted from A and C.

Alcian Blue Staining

Two wells per control (non-pressurized) and experimental (pressurized) groups were stained with alcian blue for glycosaminoglycan staining. The bottoms of the wells were photographed since photographing the cell layer was difficult due to curved surface. Based on visual inspection, the experimental group appeared to show substantial staining above the control group (Fig. 3.17).

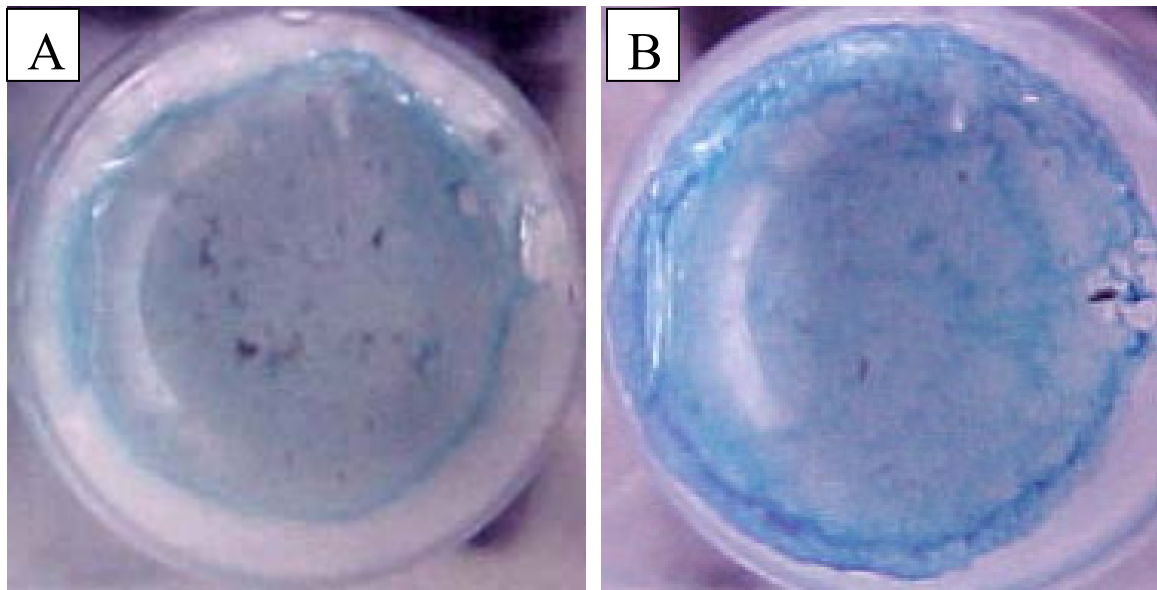


Figure 3.17 Alcian blue histochemical staining for glycosaminoglycan in samples for testing chondroinductive effect of long duration hydrostatic pressurization. (A) Control (non-pressurized) (B) Experimental (Pressurized).

Effect of Actin Disruption (by Cytochalasin D) on Chondrogenic Effects of Long Duration Hydrostatic Pressurization

This experiment was the same as the long duration hydrostatic pressurization experiment described previously except the actin cytoskeletal elements of C3H10T1/2 cells were disrupted during pressurization using Cytochalasin D. Because there was a risk of cells detaching from the substrate during the 4 hours pressurization, Cytochalasin D was used at the lower concentration of 2 μM rather than the higher concentration. While a 4 μM concentration of Cytochalasin D provides near 100% disruption of actin filaments, 2 μM provides 80% disruption, allowing cells to adhere to the substrate.

Statistical Analysis for sGAG/DNA

Sulfated glycosaminoglycan (sGAG) and DNA were quantified for 10 samples of the control (non-pressurized) and experimental groups (pressurized with Cytochalasin D). The sGAG readings ($\mu\text{g}/\text{well}$) were normalized to the respective DNA reading ($\mu\text{g}/\text{well}$) and sGAG/DNA ($\mu\text{g}/\mu\text{g}$) readings for each sample were statistically analyzed using student's t-test for two independent samples. Table 3.13 displays the result of a t-test performed to test the null hypothesis that the difference of sulfated glycosaminoglycan synthesis between the means of the populations from which the two samples come equals 0.0 versus the alternative hypothesis that the difference is not equal to 0.0. Since the P-value for this test is greater than 0.05, we cannot reject the null hypothesis at the 95.0% confidence level. Therefore, there is not a significant difference in the sGAG/DNA means of the two groups.

Comparison of Population Means					
	Sample Size	Sample Mean	Lower 95.0% Conf. Limit	Upper 95.0% Conf. Limit	Sample Std. Deviation
Control	10	0.8056	0.499783	1.11142	0.427502
Experimental	10	1.146	0.812369	1.47963	0.466382
Difference		-0.3404	-0.760727	0.0799273	
t-Test					
Null Hyp.	Alt. Hyp.	Test Statistic	P-Value		
0.0	Not equal	-1.70	0.1061		
Do not reject the null hypothesis at the 5.0% significance level.					

Table 3.13 Student's t-test for sGAG/DNA readings for control (non-pressurized) and experimental (pressurized with Cytochalasin D) samples, subjected to long duration hydrostatic pressurization.

Table 3.14 displays the results of the F-test proving the null hypothesis that the ratio of the variances of the populations from which the two samples come equals 1.0. The samples were near normal distribution as shown in Fig 3.18. Since the P-value for this test is greater than or equal to 0.05, we cannot reject the null hypothesis at the 95.0% confidence level. Therefore, both samples have equal variances.

Comparison of Population Standard Deviations				
	Sample Size	Sample Sigma	Lower 95.0% Conf. Limit	Upper 95.0% Conf. Limit
Control	10	0.427502	0.294051	0.780452
Experimental	10	0.466382	0.320794	0.851432
Ratio		0.916634	0.208698	3.38272
F Test				
Null Hyp.	Alt. Hyp.	Test Statistic	P-Value	
1.0	Not equal	0.84	0.7996	
Do not reject the null hypothesis at the 5.0% significance level.				

Table 3.14 F-test for sGAG/DNA readings for control (non-pressurized) and experimental (pressurized with Cytochalasin D) independent samples, subjected to long duration hydrostatic pressurization.

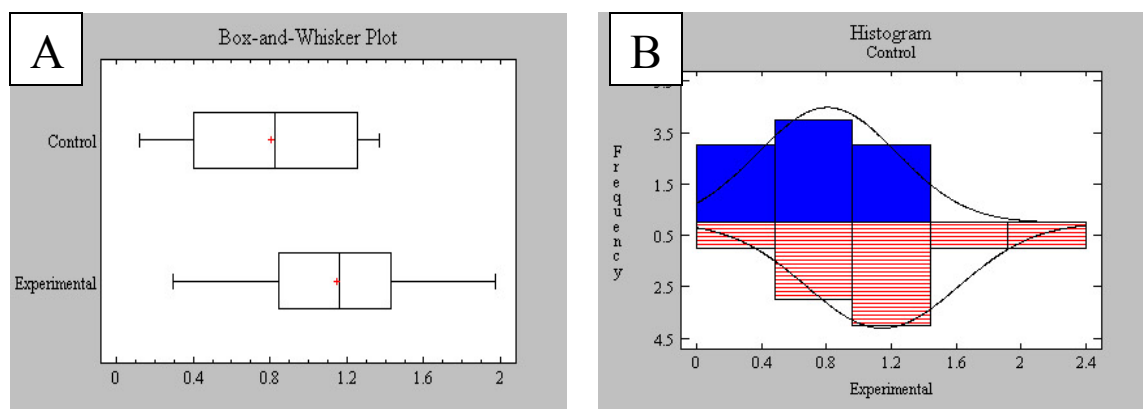


Figure 3.18 The sample distribution plots for sGAG/DNA readings comparing control (non-pressurized) and experimental (pressurized with Cytochalasin D) groups subjected to long duration hydrostatic pressure. (A) Box-and-whisker plot, (B) Histogram.

Statistical Analysis: Rate of Collagen Synthesis

The rate of collagen synthesis was quantified for 9 samples of control (non-pressurized) and experimental groups (pressurized with Cytochalasin D) by a 3H Proline radioactive assay. The scintillation reading (measured as counts per minute) for each sample was statistically analyzed using a student's t-test for the two independent samples (Table 3.15). One outlier was excluded from each group as experimental or sampling errors. An F-test was performed (Table 3.16) on the sample data to test the null hypothesis that both samples have equal variances. Since the P-value is less than 0.05, the null hypothesis was rejected proving that the variances are not equal. Since the variances are unequal, the t-test was performed using pooled variances. The obtained P-value for the t-test is less than 0.05; therefore, we must reject the null hypothesis. Since the control group had a higher sample mean than the experimental group, it was concluded that the

experimental group had a significantly lower rate of collagen synthesis as compared with the control group.

Comparison of Population Means					
	Sample Size	Sample Mean	Lower 95.0% Conf. Limit	Upper 95.0% Conf. Limit	Sample Std. Deviation
Control	8	5909.44	3620.65	8198.22	2737.71
Experimental	8	3432.9	2926.34	3939.47	605.92
Difference		2476.53	174.011	4779.05	
t-Test					
Null Hyp.	Alt. Hyp.	Test Statistic	P-Value		
0.0	Not equal	2.50	0.0382		
Reject the null hypothesis at the 5.0% significance level.					

Table 3.15 Student's t-test for radioactive counts per minute readings, comparing means for control (non-pressurized) and experimental (pressurized with Cytochalasin D) independent samples, analyzing rate of collagen synthesis of actin disrupted C3H10T1/2 cells subjected to long duration hydrostatic pressurization.

Comparison of Population Standard Deviations				
	Sample Size	Sample Sigma	Lower 95.0% Conf. Limit	Upper 95.0% Conf. Limit
Control	8	2737.71	1810.1	5571.98
Experimental	8	605.92	400.619	1233.21
Ratio		4.51826	4.0871	101.97
F Test				
Null Hyp.	Alt. Hyp.	Test Statistic	P-Value	
1.0	Not equal	20.41	0.0007	
Reject the null hypothesis at the 5.0% significance level.				

Table 3.16 F-test for radioactive counts per minute readings, comparing population standard deviations for control (non-pressurized) and experimental (pressurized with Cytochalasin D) independent samples, analyzing rate of collagen synthesis of actin disrupted C3H10T1/2 cells subjected to long duration hydrostatic pressurization.

Collagen Type II Immunostaining

Two wells per control (non-pressurized) and experimental (pressurized) groups were stained with II-II6B3 antibody for type II collagen. One well per group was not stained with the antibody and was treated as the control for immunostaining. Fig. 3.19 shows the results from this assay.

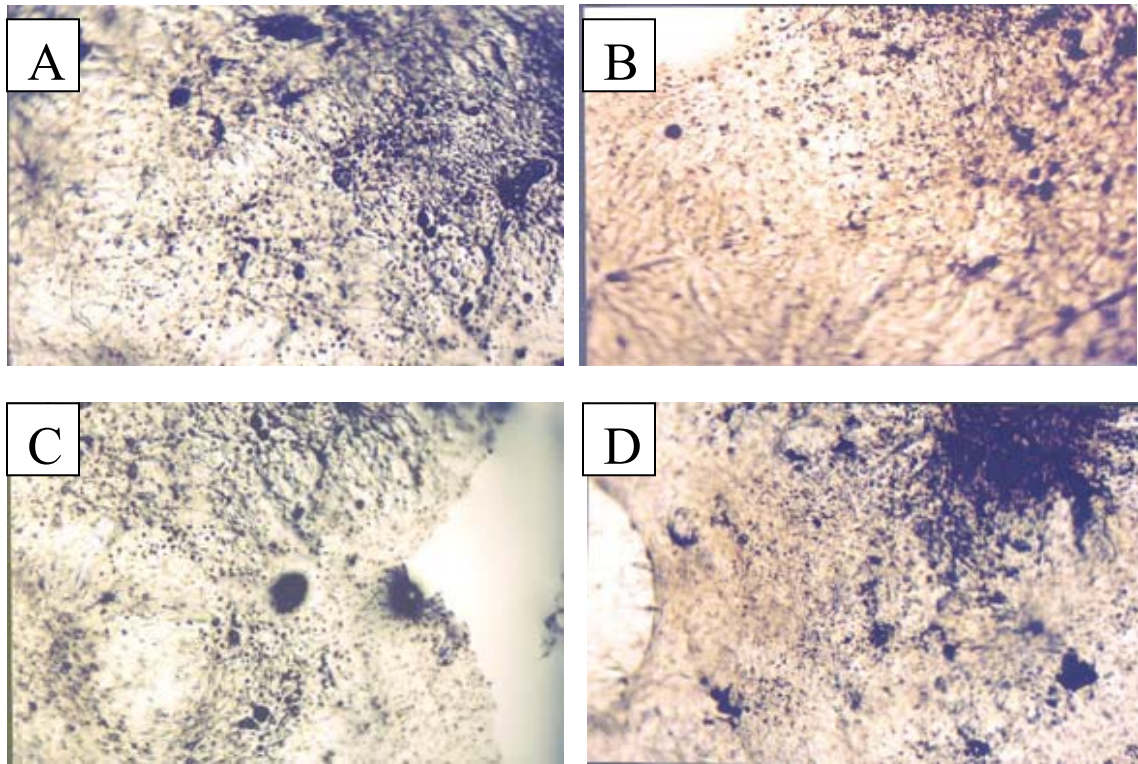


Figure 3.19 Collagen type II immunostaining in micromass cultures of Cytochalasin D treated C3H/10T1/2 cells hydrostatically pressurized for long duration (4X). A-B: Control, C-D: pressurized. Primary antibody was omitted from A and C.

Alcian Blue Staining

Two wells per control (non-pressurized) and experimental (pressurized) groups were stained with alcian blue for glycosaminoglycan staining. The bottoms of the wells were photographed since photographing the cell layer was difficult due to curved surface. There was no visual difference in the alcian blue staining between the control and the experimental samples (Fig. 3.20).

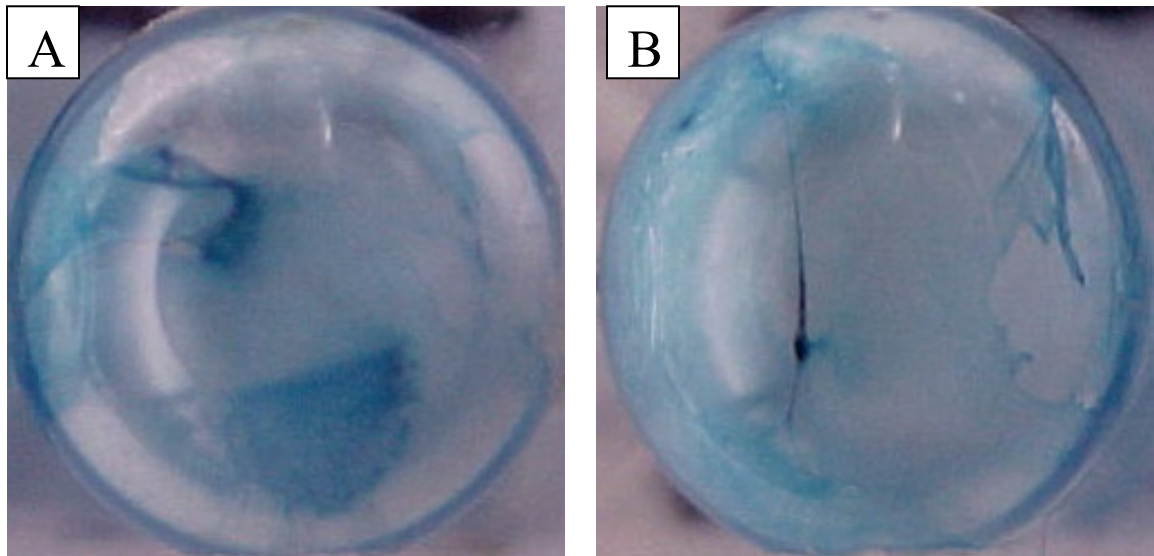


Figure 3.20 Alcian blue histochemical staining for glycosaminoglycan in samples for testing chondroinductive effect of long duration hydrostatic pressurization with actin cytoskeleton elements disrupted using Cytochalasin D. (A) Control (non-pressurized) (B) Experimental (Pressurized with Cytochalasin D).

CHAPTER IV

DISCUSSION AND CONCLUSION

This study has examined the role of the actin cytoskeletal filaments disrupting agent, Cytochalasin D, on hydrostatic pressure induced chondrogenic differentiation of C3H10T1/2 mesenchymal stem cells. The effect of Cytochalasin D on actin disruption was characterized for cytotoxicity, concentration, duration of exposure and reversibility. Although, Cytochalasin D is known to induce actin filament disruption even at very low concentrations (Zanetti and Solursh, 1984), a concentration of 4 μM disrupts the actin filaments almost completely with 2 hours of treatment. Cytochalasin D was not shown to have any toxicity effects on C3H10T1/2 cells. The cells proliferated substantially during the 2 hour per day treatment with Cytochalasin D which was evident by the reversible actin disruption noted after the treatment. The cells were found to regain and reorganize the actin cytoskeletal structure within 6-8 hours after drug removal.

To avoid confusion on chondroinduction in hydrostatic pressurization experiments, the effect of the actin disruption due to Cytochalasin D on chondrogenesis of C3H10T1/2 was examined. In early studies, C3H/10T1/2 cells have been shown to express the myocyte, adipocyte and chondrocyte phenotypes after treatment with azacytidine [Taylor and Jones, 1979], and have subsequently been shown to be capable of

selective differentiation to these, as well as the osteoblast phenotype [Atkinson et al., 1997; Chen et al., 2001; Bartsch et al., 2000]. Denker et al. [1999] reported that chondrogenic differentiation of C3H/10T1/2 occurred when plated as high-density micromass and treated with 10-100 ng/ml rhBMP-2. These culture conditions were adopted for the present study, and chondrocyte differentiation due to rhBMP-2 was confirmed by metachromatic staining with toluidine blue and the accumulation of substantial sGAG. The chondrogenic effect of Cytochalasin D was tested in micromass culture and was compared with BMP-2 induced chondrogenesis. The toluidine blue staining and sGAG assay show that there was no chondroinductive effect due to actin disruption alone and no enhancement of BMP-2 mediated chondroinduction.

Cytochalasin D stimulated chondroinduction in chick limb bud cells has been reported by Zanetti and Solursh (1984). These results contradict with results obtained in the current studies and can be explained by the time of exposure of the cells to Cytochalasin D. Zanetti and Solursh have identified that the chondroinduction occurs only during the treatment with the drug in the first 24 hour treatment from the time of seeding. In this study, we exposed the cells to the drug after the first 24 hours so as to comply with the experimental design of cyclic hydrostatic pressurization where the first 24 hours are allowed for proper cell attachment to substrate. The contradiction may also be attributed to the difference in species, to the use of a transformed cell line, or to the relative homogeneity of the cell line as compared to chick limb bud cells.

To examine the role of actin cytoskeletal filaments disrupting agent, Cytochalasin D, on hydrostatic pressure induced chondrogenic differentiation, it was important to

characterize cyclic hydrostatic pressure as a chondroinductive model. The capacity for the mechanical environment to influence chondrocyte differentiation, such as that which occurs during limb formation, has been established. Takahashi et al. [1998] found transcriptional upregulation of cartilage-specific genes in mouse limb bud cells within a collagen gel matrix exposed to static compressive force, and Elder et al. [2000] reported enhanced chondrogenesis of agarose-embedded limb bud cells subjected to cyclic unconfined compression. However, due to the static nature of the load in the former and the high permeability of agarose in the latter, it is unlikely that hydrostatic pressure was the primary chondrogenic stimulus in either of these studies. While the importance of hydrostatic pressure, relative to other modes of loading, in maintaining the chondrocyte phenotype has been demonstrated [Wong et al., 2002], much remains to be determined regarding the potential for hydrostatic pressure to induce chondrocyte differentiation.

This study demonstrates the use of a custom apparatus for applying cyclic hydrostatic compression to cells in vitro. Hydrostatic pressure was transferred to C3H/10T1/2 murine embryo fibroblasts growing in high-density culture in portions of a 96-well round-bottom polystyrene plate. The extensive cell-cell contact facilitated by the micromass culture technique is somewhat representative of the in vivo situation in which chondrocyte differentiation during limb formation is preceded by mesenchymal cell condensation. Cell-cell contact may also be an important contributor to the ability of a cell population to respond to mechanical stress. Other experiments done by Dr. Steven H. Elder have revealed that the response of chondrocyte aggregates to cyclic hydrostatic

compression is significantly greater than that of their alginate-embedded counterparts (unpublished data).

The magnitude and frequency of the applied pressure were chosen to be within the physiological range [Mow et al., 1992] and which have previously been demonstrated to stimulate cartilaginous matrix production in vitro [Ikenoue et al., 2003]. Loading was applied only during the initial three days of culture to isolate its effect on the chondrogenic commitment of cells to the chondrogenic lineage. Extending the loading period may have had an anabolic effect on chondrocytic cells. For short duration studies, each daily loading session lasted 50 minutes (three 10-minute loading periods separated by two 10-minute rest intervals). For long duration studies, the cells were pressurized for 4 hours per day with 10 minutes of pressurization and 10 minutes of a rest cycle. A total of 7200 cycles were applied on each of 3 consecutive days. This scheme allowed sufficient time for cells to respond as Bachrach et al. [1995] have shown that cartilage explants subjected to 0.1 MPa stress for 10 minutes, during which time the load is mainly supported by fluid pressure, stimulated glycosaminoglycan synthesis by 57%.

Short duration cyclic hydrostatic pressure from 0.3 to 5.0 MPa at 1 Hz applied for 30 minutes a day (1800 cycles) for three days did not alter DNA content and did not enhance chondroinduction of C3H/10T1/2 cells by rhBMP-2. Angele et al. [2003] similarly observed no effect of cyclic hydrostatic compression on aggregates of human bone marrow-derived mesenchymal progenitor cells if applied for 4 h on a single day. However, the application of pressure for 4 h per day for seven consecutive days enhanced cartilaginous matrix formation but did not change DNA content in the same model.

Likewise, Mauk et al. [2003] demonstrated increased expression of aggrecan mRNA and greater pericellular type II collagen in human bone marrow mesenchymal cells embedded in alginate and pressurized to ~3 MPa at 0.33 Hz for one hour per day, five days per week for two weeks. The lack of response in the current study may be attributed to the fewer number of loading cycles experienced each day and/or to the fewer number of days over which the cells were loaded. Therefore the number of cycles was increased to 7200 cycles per day in long duration cyclic hydrostatic pressurization. Increasing the number of cycles increased sulfated glycosaminoglycan, and the rate of collagen synthesis, but did not change DNA content. These results are consistent with previous findings that the response of chondrocytes to cyclic hydrostatic compression is time-dependent, increasing with duration up to several hours [Angele et al., 2003; Smith et al., 2000; Parkkinen et al., 1993]. The concept that the cells should be loaded for more days suggests that mesenchymal stem cells are sensitive to the cumulative hydrostatic stress history (over a multi-day period); a concept that has also previously been demonstrated for chondrocytes [Ikenoue et al., 2003; Ellison et al., 1994]. For a given pressure waveform applied on a daily basis, a duration (number of cycles) threshold that must be exceeded to elicit a chondrogenic response may exist. For example, Nagatomi et al. [2001] reported that osteoblast proliferation was decreased by exposure to cyclic pressure at 1.0 Hz for 1 h daily for 5 days, but was not affected by the same pressure applied for only 20 min per day.

This study did not address the possibility that hydrostatic pressurization could induce chondrocyte differentiation in the absence of rhBMP-2. The aforementioned

experiments by Angele et al. [2003] were also all conducted in the presence of chondroinductive transforming growth factor beta-3. Mauk et al. [2003], however, did report an approximate 40% increase in the relative gene expression of aggrecan associated with dynamic hydrostatic pressure alone, which was increased to approximately 150% in the presence of transforming growth factor beta-1. Therefore, it is possible that hydrostatic pressure could trigger commitment to the chondrocyte lineage, as well as promote matrix macromolecule formation, but further studies are necessary to clarify this issue.

Disrupting actin filaments using Cytochalasin D during the long duration cyclic hydrostatic pressure did not alter DNA content nor enhance sulfated glycosaminoglycan synthesis above the mean level of the non-pressurized group. The diminished chondroinductive effect of long duration cyclic hydrostatic pressurization in the presence of Cytochalasin D indicates that the actin cytoskeletal elements play a critical role in the mechanotransduction of cyclic hydrostatic pressure induced chondroinduction. Although, the cell signaling mechanism for Cytochalasin D is not yet fully known, it has been demonstrated that Cytochalasin D is involved with a few cell signaling pathways like protein kinase C (PKC), NO, and extracellular signal-regulated protein kinase (Erk-1) [Lim et al., 2000; Kim et al., 2003].

Disruption of actin filaments was found to inhibit sGAG synthesis in the chondroinductive hydrostatic pressurization environment. However, it significantly inhibited hydrostatic-pressurization-induced rate of collagen synthesis to the mean level

lower than that of the non-pressurized group. This again can be attributed to the effect of actin disruption on the intracellular signaling.

In conclusion, this study found no influence, in terms of chondrogenesis, of three days exposure of Cytochalasin D treated C3H/10T1/2 mesenchymal stem cells to 7200 cycles/day of dynamic hydrostatic pressure to 5.0 MPa. However, the rate of collagen synthesis was inhibited in the process. This finding indicates that the actin cytoskeletal elements play a critical role in the mechanotransduction of cyclic hydrostatic pressure induced chondroinduction.

Understanding the structural role and signal transduction mechanisms of actin filaments may provide a regulatory mechanism for mesenchymal cell differentiation into developing cartilage tissue or cartilage tissue engineering by physical stimulation.

REFERENCES CITED

- [1] Angele, P., Yoo, J.U., Smith, C., Mansour, J., Jepsen, K.J., Nerlich, M., Johnstone, B. (2003); Cyclic hydrostatic pressure enhances the chondrogenic phenotype of human mesenchymal progenitor cells differentiated in vitro. *J Orthop Res.*; 21(3): 451-7.
- [2] Atkinson, B.L., Fantle, K.S., Benedict, J.J., Huffer, W.E., Gutierrez-Hartmann, A. (1997); Combination of osteoinductive bone proteins differentiates mesenchymal C3H/10T1/2 cells specifically to the cartilage lineage. *J Cell Biochem.*; 65(3): 325-39.
- [3] Bachrach, N.M., Valhmu, W.B., Stazzone, E., Ratcliffe, A., Lai, W.M., Mow, V.C. (1995); Changes in proteoglycan synthesis of chondrocytes in articular cartilage are associated with the time-dependent changes in their mechanical environment. *J Biomech*; 28(12): 1561-9.
- [4] Bartsch, J.W., Jackel, M., Perz, A., Jockusch, H. (2000); Steroid RU 486 inducible myogenesis by 10T1/2 fibroblastic mouse cells. *FEBS Lett.* 4; 467(1): 123-7.
- [5] Bonassar, L.J., Grodzinsky, A.J., Frank, E.H., Davila, S.G., Bhaktav, N.R., Trippel, S.B. (2001); The effect of dynamic compression on the response of articular cartilage to insulin-like growth factor-I. *J Orthop Res.*; 19(1): 11-7.
- [6] Boudreau, N., Bissell, M.J. (1998); Extracellular matrix signaling: integration of form and function in normal and malignant cells. *Curr Opin Cell Biol.*; 10(5): 640-6.

- [7] Burdick, J.A., Anseth, K.S. (2002); Photoencapsulation of osteoblasts in injectable RGD-modified PEG hydrogels for bone tissue engineering. *Biomaterials*. 2002 Nov; 23(22): 4315-23.
- [8] Buschmann, M.D., Hunziker, E.B., Kim, Y.J., Grodzinsky, A.J. (1996); Altered aggrecan synthesis correlates with cell and nucleus structure in statically compressed cartilage. *J Cell Sci.*; 109 (Pt 2): 499-508.
- [9] Carter, D.R., Wong, M. (2003); Modelling cartilage mechanobiology. *Philos Trans R Soc Lond B Biol Sci.*; 358(1437): 1461-71.
- [10] Carver, S.E., Heath, C.A. (1999); Increasing extracellular matrix production in regenerating cartilage with intermittent physiological pressure. *Biotechnol Bioeng.*; 62(2): 166-74.
- [11] Chen, T.L., Shen, W.J., Kraemer, F.B. (2001); Human BMP-7/OP-1 induces the growth and differentiation of adipocytes and osteoblasts in bone marrow stromal cell cultures. *J Cell Biochem.*; 82(2): 187-99.
- [12] Chicurel, M.E., Chen, C.S., Ingber, D.E. (1998); Cellular control lies in the balance of forces. *Curr Opin Cell Biol.*; 10(2): 232-9.
- [13] Dean, D., Topham, N.S., Rimnac, C., Mikos, A.G., Goldberg, D.P., Jepsen, K., Redtfeldt, R., Liu, Q., Pennington, D., Ratcheson, R. (1999); Osseointegration of preformed polymethylmethacrylate craniofacial prostheses coated with bone marrow-impregnated poly (DL-lactic-co-glycolic acid) foam. *Plast Reconstr Surg.*; 104(3): 705-12.
- [14] Denker, A.E., Haas, A.R., Nicoll, S.B., Tuan, R.S. (1999); Chondrogenic differentiation of murine C3H10T1/2 multipotential mesenchymal cells: I. Stimulation by bone morphogenetic protein-2 in high-density micromass cultures. *Differentiation*; 64(2): 67-76.
- [15] Durrant, L.A., Archer, C.W., Benjamin, M., Ralphs, J.R. (1999); Organisation of the chondrocyte cytoskeleton and its response to changing mechanical conditions in organ culture. *J Anat.*; 194 (Pt 3): 343-53.

- [16] Elder, S.H., Kimura, J.H., Soslowky, L.J., Lavagnino, M., Goldstein, S.A. (2000); Effect of compressive loading on chondrocyte differentiation in agarose cultures of chick limb-bud cells. *J Orthop Res.*; 18(1): 78-86.
- [17] Elder, S.H., Goldstein, S.A., Kimura, J.H., Soslowky, L.J., Spengler, D.M. (2001); Chondrocyte differentiation is modulated by frequency and duration of cyclic compressive loading. *Ann Biomed Eng.*; 29(6): 476-82.
- [18] Ellison, B.E., Carter, D.R., Smith, R.L. (1994); Effect of variable duration intermittent hydrostatic pressure on cartilage glycoaminoglycan synthesis. *Trans Orthop Res Soc.*; 19: 486.
- [19] Frank, E.H., Grodzinsky, A.J. (1987); Cartilage electromechanics--I. Electrokinetic transduction and the effects of electrolyte pH and ionic strength. *J Biomech.*; 20(6): 615-27.
- [20] Frank, E.H., Grodzinsky, A.J. (1987); Cartilage electromechanics--II. A continuum model of cartilage electrokinetics and correlation with experiments. *J Biomech.*; 20(6): 629-39.
- [21] Garofalo, S., Metsaranta, M., Ellard, J., Smith, C., Horton, W., Vuorio, E., de Crombrughe, B. (1993); Assembly of cartilage collagen fibrils is disrupted by overexpression of normal type II collagen in transgenic mice. *Proc Natl Acad Sci.*; 90(9): 3825-9.
- [22] Gray, M.L., Pizzanelli, A.M., Grodzinsky, A.J., Lee, R.C. (1988); Mechanical and physiochemical determinants of the chondrocyte biosynthetic response. *J Orthop Res.*; 6(6): 777-92.
- [23] Griffith, L.G., Wu, B., Cima, M.J., Powers, M.J., Chaignaud, B., Vacanti, J.P. (1997); In vitro organogenesis of liver tissue. *Ann N Y Acad Sci.*; 831: 382-97.
- [24] Guilak, F., Ratcliffe, A., Mow, V.C. (1995); Chondrocyte deformation and local tissue strain in articular cartilage: a confocal microscopy study. *J Orthop Res.*; 13(3): 410-21.

- [25] Guilak, F., Tedrow, J.R., Burgkart, R. (2000) Viscoelastic properties of the cell nucleus. *Biochem Biophys Res Commun.*; 269(3): 781-6.
- [26] Guilak, F., Erickson, G.R., Ting-Beall, H.P. (2002); The effects of osmotic stress on the viscoelastic and physical properties of articular chondrocytes. *Biophys J.*; 82(2): 720-7.
- [27] Haas, A.R., Tuan, R.S. (1999); Chondrogenic differentiation of murine C3H10T1/2 multipotential mesenchymal cells: II. Stimulation by bone morphogenetic protein-2 requires modulation of N-cadherin expression and function. *Differentiation*; 64: 77-89.
- [28] Hall, A.C. (1999); Differential effects of hydrostatic pressure on cation transport pathways of isolated articular chondrocytes. *J Cell Physiol.* 178(2): 197-204.
- [29] Idowu, B.D., Knight, M.M., Bader, D.L., Lee, D.A. (2000); Confocal analysis of cytoskeletal organisation within isolated chondrocyte sub-populations cultured in agarose. *Histochem J.*; 32(3): 165-74.
- [30] Ikenoue, T., Trindade, M.C., Lee, M.S., Lin, E.Y., Schurman, D.J., Goodman, S.B., Smith, R.L. (2003); Mechanoregulation of human articular chondrocyte aggrecan and type II collagen expression by intermittent hydrostatic pressure in vitro. *J Orthop Res.*; 21(1): 110-6.
- [31] Ingber, D.E. (1997); Tensegrity: the architectural basis of cellular mechanotransduction. *Annu Rev Physiol.*; 59: 575-99.
- [32] Jin, M., Frank, E.H., Quinn, T.M., Hunziker, E.B., Grodzinsky, A.J. (2001); Tissue shear deformation stimulates proteoglycan and protein biosynthesis in bovine cartilage explants. *Arch Biochem Biophys.*; 395(1): 41-8.
- [33] Jortikka, M.O., Parkkinen, J.J., Inkinen, R.I., Karner, J., Jarvelainen, H.T., Nelimarkka, L.O., Tammi, M.I., Lammi, M.J. (2000) The role of microtubules in the regulation of proteoglycan synthesis in chondrocytes under hydrostatic pressure. *Arch Biochem Biophys.*; 374(2): 172-80.

- [34] Karjalainen, H.M., Sironen, R.K., Elo, M.A., Kaarniranta, K., Takigawa, M., Helminen, H.J., Lammi, M.J. (2003); Gene expression profiles in chondrosarcoma cells subjected to cyclic stretching and hydrostatic pressure. A cDNA array study. *Biorheology.*; 40(1-3): 93-100.
- [35] Kim, B.S., Nikolovski, J., Bonadio, J., Mooney, D.J. (1999); Cyclic mechanical strain regulates the development of engineered smooth muscle tissue. *Nat Biotechnol.*; 17(10): 979-83.
- [36] Kim, S.J., Hwang, S.G., Kim, I.C., Chun, J.S. (2003); Actin cytoskeletal architecture regulates nitric oxide-induced apoptosis, dedifferentiation, and cyclooxygenase-2 expression in articular chondrocytes via mitogen-activated protein kinase and protein kinase C pathways. *J Biol Chem.*; 278(43): 42448-56.
- [37] Kim, Y.J., Sah, R.L., Grodzinsky, A.J., Plaas, A.H., Sandy, J.D. (1994); Mechanical regulation of cartilage biosynthetic behavior: physical stimuli. *Arch Biochem Biophys.*; 311(1): 1-12.
- [38] Kim, Y.J., Bonassar, L.J., Grodzinsky, A.J. (1995); The role of cartilage streaming potential, fluid flow and pressure in the stimulation of chondrocyte biosynthesis during dynamic compression. *J Biomech.*; 28(9): 1055-66.
- [39] Koyano, Y., Hammerle, H., Mollenhauer, J. (1997); Analysis of 3H-proline-labeled protein by rapid filtration in multiwell plates for the study of collagen metabolism. *Biotechniques.*; 22(4): 706-8, 710-2, 714 passim.
- [40] Lai, W.M., Hou, J.S., Mow, V.C. (1991); A triphasic theory for the swelling and deformation behaviors of articular cartilage. *J Biomech Eng.*; 113(3): 245-58.
- [41] Langelier, E., Suetterlin, R., Hoemann, C.D., Aebi, U., Buschmann, M.D. (2000); The chondrocyte cytoskeleton in mature articular cartilage: structure and distribution of actin, tubulin, and vimentin filaments. *J Histochem Cytochem.*; 48(10): 1307-20.

- [42] Lee, D.A., Knight, M.M., Bolton, J.F., Idowu, B.D., Kayser, M.V., Bader, D.L. (2000); Chondrocyte deformation within compressed agarose constructs at the cellular and sub-cellular levels. *J Biomech.*; 33(1): 81-95.
- [43] Lim, Y.B., Kang, S.S., Park, T.K., Lee, Y.S., Chun, J.S., Sonn, J.K. (2000); Disruption of actin cytoskeleton induces chondrogenesis of mesenchymal cells by activating protein kinase C-alpha signaling. *Biochem Biophys Res Commun.*; 273(2): 609-13.
- [44] Lysaght, M.J. and O'Loughlin, J. A. (2000); Demographic scope and economic magnitude of contemporary organ therapies. *ASAIO Journal* 46: 515-521.
- [45] Mauck, R.L., Oswald, E.S., Cheng, Q., Majumdar, M.K., Nicoll, S.B., Ateshian, G.A., Hung, C.T. (2003); Hydrostatic pressure enhances chondrogenic differentiation of human multipotential mesenchymal cells in alginate disks. *Trans ASME Summer Bioengineering Conference*: 265-266.
- [46] Meazzini, M.C., Toma, C.D., Schaffer, J.L., Gray, M.L., Gerstenfeld, L.C. (1998); Osteoblast cytoskeletal modulation in response to mechanical strain in vitro. *J Orthop Res.*; 16(2): 170-80.
- [47] Minguell, J.J., Erices, A., Conget, P. (2001); Mesenchymal stem cells. *Exp Biol Med (Maywood)*. 226(6): 507-20.
- [48] Mooney, D.J. and Mikos, A.G. (1999); Growing new organs. *Scientific American*; 280(4): 60-5.
- [49] Mow, V.C., Kuei, S.C., Lai, W.M., Armstrong, C.G. (1980); Biphasic creep and stress relaxation of articular cartilage in compression? Theory and experiments. *J Biomech Eng.*; 102(1): 73-84.
- [50] Mow, V.C., Ratcliffe, A., Poole, A.R. (1992); Cartilage and diarthrodial joints as paradigms for hierarchical materials and structures. *Biomaterials*; 13(2): 67-97.

- [51] Nagatomi, J., Arulanandam, B.P., Metzger, D.W., Meunier, A., Bizios, R. (2001); Frequency- and duration-dependent effects of cyclic pressure on select bone cell functions. *Tissue Eng.*; 7(6): 717-28.
- [52] Osborn, M. and Weber, K. (1977); The display of microtubules in transformed cells. *Cell*; 12(3): 561-71.
- [53] Parkkinen, J.J., Ikonen, J., Lammi, M.J., Laakkonen, J., Tammi, M., Helminen, H.J. (1993); Effects of cyclic hydrostatic pressure on proteoglycan synthesis in cultured chondrocytes and articular cartilage explants. *Arch Biochem Biophys.*; 300(1): 458-65.
- [54] Puelacher, W.C., Mooney, D., Langer, R., Upton, J., Vacanti, J.P., Vacanti, C.A. (1994); Design of nasoseptal cartilage replacements synthesized from biodegradable polymers and chondrocytes. *Biomaterials*; 15(10): 774-8.
- [55] Putnam, A.J., Schultz, K., Mooney, D.J. (2001); Control of microtubule assembly by extracellular matrix and externally applied strain. *Am J Physiol Cell Physiol.*; 280(3): C556-64.
- [56] Roark, E.F. and Greer, K. (1994); Transforming growth factor-beta and bone morphogenetic protein-2 act by distinct mechanisms to promote chick limb cartilage differentiation in vitro. *Dev Dyn.*; 200(2): 103-16.
- [57] Sah, R.L., Kim, Y.J., Doong, J.Y., Grodzinsky, A.J., Plaas, A.H., Sandy, J.D. (1989); Biosynthetic response of cartilage explants to dynamic compression. *J Orthop Res.*; 7(5): 619-36.
- [58] Salter, D.M., Millward-Sadler, S.J., Nuki, G., Wright, M.O. (2001); Integrin-interleukin-4 mechanotransduction pathways in human chondrocytes. *Clin Orthop.*; (391 Suppl): S49-60.
- [59] Sato, M., Ochi, T., Nakase, T., Hirota, S., Kitamura, Y., Nomura, S., Yasui, N. (1999); Mechanical tension-stress induces expression of bone morphogenetic protein (BMP)-2 and BMP-4, but not BMP-6, BMP-7, and

GDF-5 mRNA, during distraction osteogenesis. *J Bone Miner Res.*; 14(7): 1084-95.

- [60] Shieh, A.C. and Athanasiou, K.A. (2003); Principles of cell mechanics for cartilage tissue engineering. *Ann Biomed Eng.*; 31(1): 1-11.
- [61] Smith, R.L., Donlon, B.S., Gupta, M.K., Mohtai, M., Das, P., Carter, D.R., Cooke, J., Gibbons, G., Hutchinson, N., Schurman, D.J. (1995); Effects of fluid-induced shear on articular chondrocyte morphology and metabolism in vitro. *J Orthop Res.*; 13(6): 824-31.
- [62] Smith, R.L., Rusk, S.F., Ellison, B.E., Wessells, P., Tsuchiya, K., Carter, D.R., Caler, W.E., Sandell, L.J., Schurman, D.J. (1996); In vitro stimulation of articular chondrocyte mRNA and extracellular matrix synthesis by hydrostatic pressure. *J Orthop Res.*; 14(1): 53-60.
- [63] Smith, R.L., Lin, J., Trindade, M.C., Shida, J., Kajiyama, G., Vu, T., Hoffman, A.R., van der Meulen, M.C., Goodman, S.B., Schurman, D.J., Carter, D.R. (2000); Time-dependent effects of intermittent hydrostatic pressure on articular chondrocyte type II collagen and aggrecan mRNA expression. *J Rehabil Res Dev.*; 37(2): 153-61.
- [64] Takahashi, I., Nuckolls, G.H., Takahashi, K., Tanaka, O., Semba, I., Dashner, R., Shum, L., Slavkin, H.C. (1998); Compressive force promotes sox9, type II collagen and aggrecan and inhibits IL-1beta expression resulting in chondrogenesis in mouse embryonic limb bud mesenchymal cells. *J Cell Sci.*; 111 (Pt 14): 2067-76.
- [65] Takahashi, I., Onodera, K., Sasano, Y., Mizoguchi, I., Bae, J.W., Mitani, H., Kagayama, M., Mitani, H. (2003); Effect of stretching on gene expression of beta1 integrin and focal adhesion kinase and on chondrogenesis through cell-extracellular matrix interactions. *Eur J Cell Biol.*; 82(4): 182-92.
- [66] Taylor, S.M. and Jones, P.A. (1979); Multiple new phenotypes induced in 10T1/2 and 3T3 cells treated with 5-azacytidine. *Cell*; 17(4): 771-9.

- [67] Tumminia, S.J., Mitton, K.P., Arora, J., Zelenka, P., Epstein, D.L., Russell, P. (1998); Mechanical stretch alters the actin cytoskeletal network and signal transduction in human trabecular meshwork cells. *Invest Ophthalmol Vis Sci.*; 39(8): 1361-71.
- [68] van der Kraan, P.M. and van den Berg, W.B. (2000); Anabolic and destructive mediators in osteoarthritis. *Curr Opin Clin Nutr Metab Care.*; 3(3): 205-11.
- [69] Vunjak-Novakovic, G., Martin, I., Obradovic, B., Treppo, S., Grodzinsky, A.J., Langer, R., Freed, L.E. (1999); Bioreactor cultivation conditions modulate the composition and mechanical properties of tissue-engineered cartilage. *J Orthop Res.*; 17(1): 130-8.
- [70] Wang, N., Butler, J.P., Ingber, D.E. (1993); Mechanotransduction across the cell surface and through the cytoskeleton. *Science*; 260(5111): 1124-7.
- [71] Wong, M., Siegrist, M., Goodwin, K., Park, Y. (2002); Hydrostatic pressure, tension and unconfined compression differentially regulate expression of cartilage matrix proteins. *Trans Orthop Res Soc*; 27: 33.
- [72] Zanetti, N.C., Solursh, M. (1984); Induction of chondrogenesis in limb mesenchymal cultures by disruption of the actin cytoskeleton. *J Cell Biol.*; 99(1 Pt 1): 115-23.

APPENDIX

A. HYDROSTATIC PRESSURIZATION DEVICE

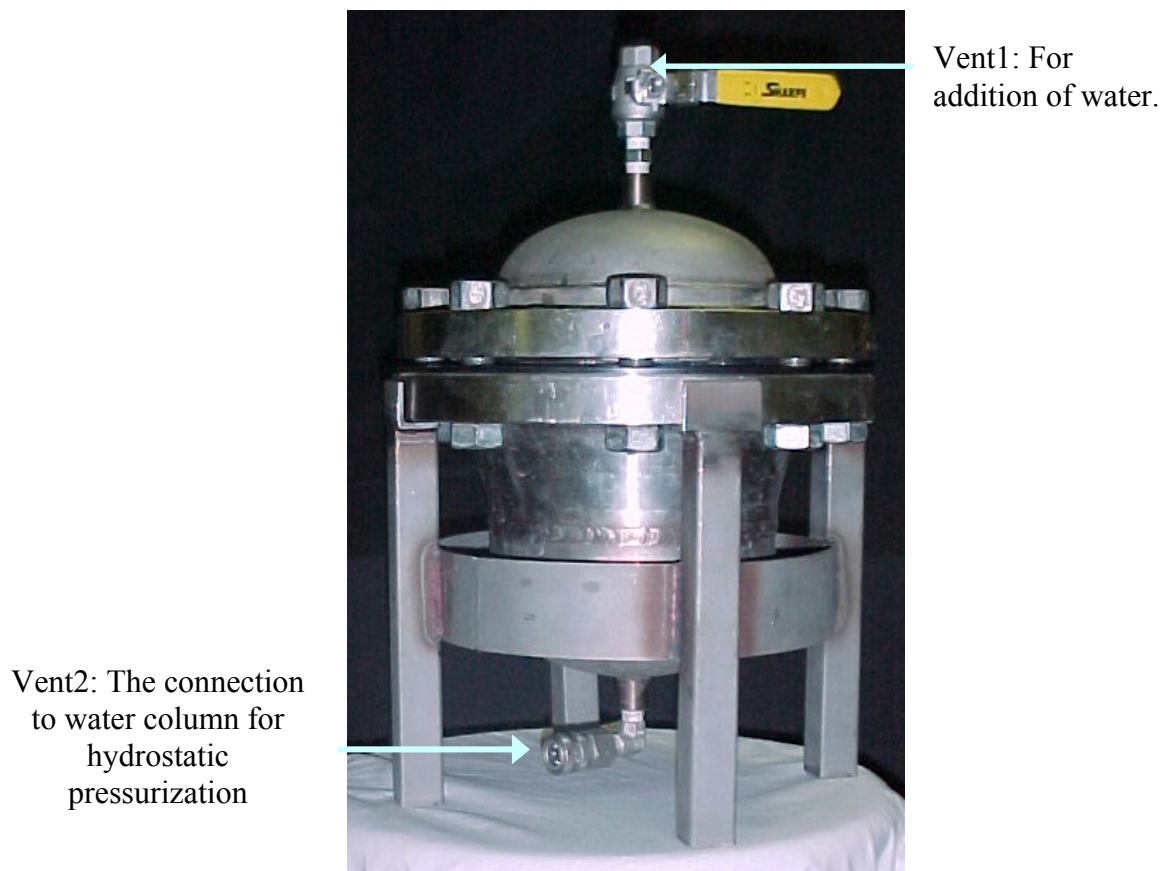


Figure A.1 The hydrostatic pressurization chamber.

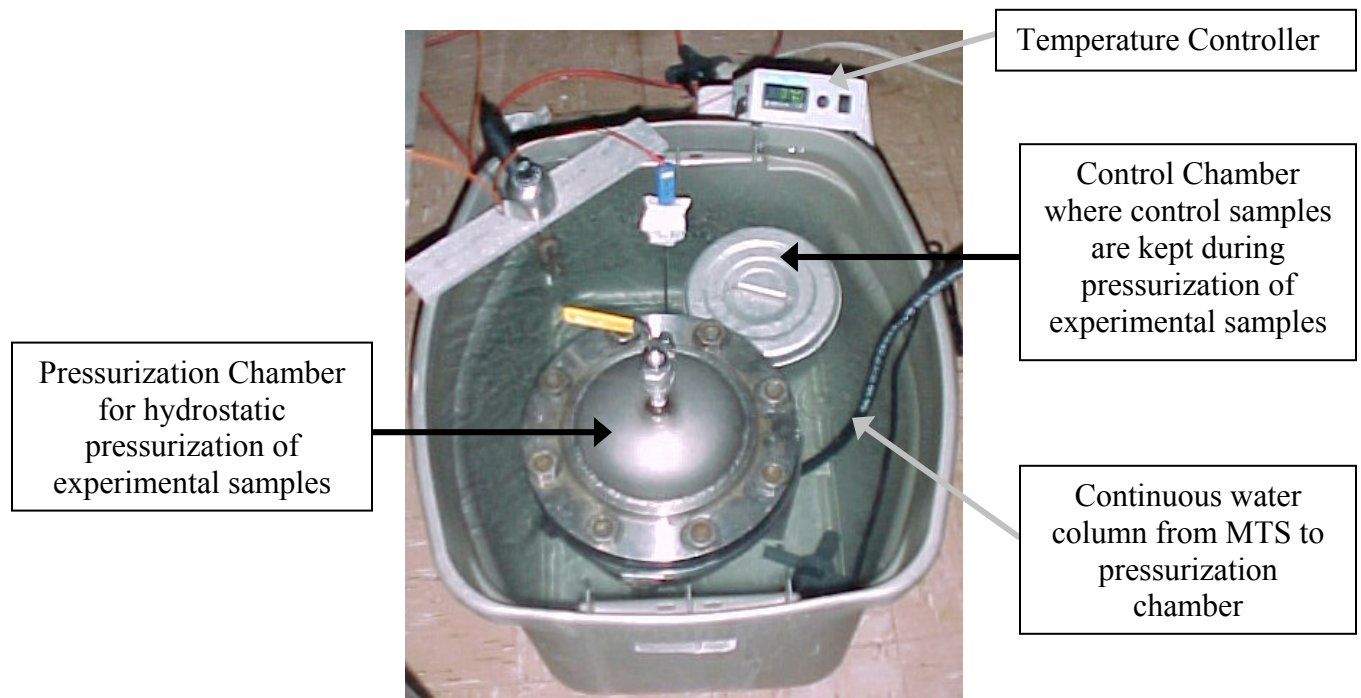


Figure A.2 The hydrostatic pressurization chamber and control chamber was maintained in water bath at 37°C during pressurization.

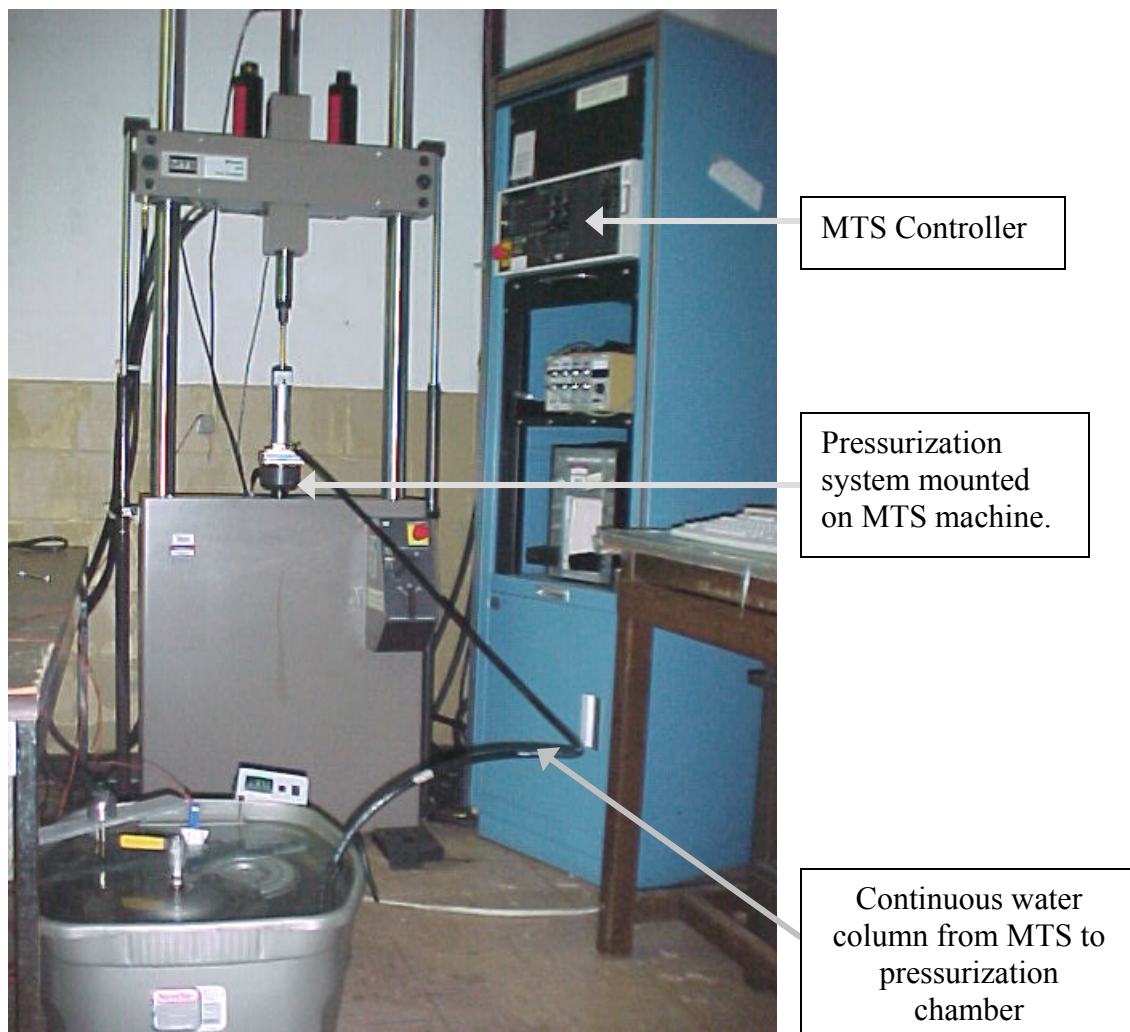


Figure A.3 The overall setup of hydrostatic pressurization chamber with MTS machine controlled pressurization. Continuous water column was maintained from MTS machine to the pressurization chamber.